Aggregation model and related topics

Theodore Kolokolnikov

Dalhousie University

Aggregation model

We consider a simple model of particle interaction,

$$\frac{dx_j}{dt} = \frac{1}{N} \sum_{\substack{k=1\ldots N \\ k\neq j}} F\left(|x_j - x_k|\right) \frac{x_j - x_k}{|x_j - x_k|}, \quad j = 1 \ldots N \tag{1}$$

- Models insect aggregation [Edelstein-Keshet et al, 1998] such as locust swarms [Topaz et al, 2008]; robotic motion [Gazi, Passino, 2004].
- Interaction force $F(r)$ is of ***attractive-repelling type***: the insects repel each other if they are too close, but attract each-other at a distance.
- Note that acceleration effects are ignored as a first-order approximation.
- Mathematically $F(r)$ is positive for small r, but negative for large r.
- Alternative formulation: (1) is a gradient flow of the minimization problem

$$\min E\left(x_1, \ldots x_N\right) \quad \text{where} \quad E = \sum \sum P(|x_i - x_j|) \quad \text{with} \quad F(r) = -P'(r).$$

Confining vs. spreading

- Consider a ***Morse interaction force***:

$$F(r) = \exp(-r) - G\exp(-r/L); \quad G < 1, L > 1 \tag{2}$$

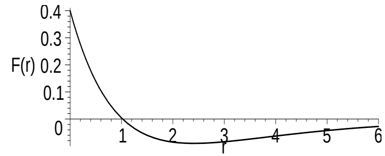

- If $GL^3 > 1$, the morse potential is ***confining*** (or catastrophic): doubling N doubles the density but cloud volume is unchanged:

$$G = 0.5, \quad L = 2$$

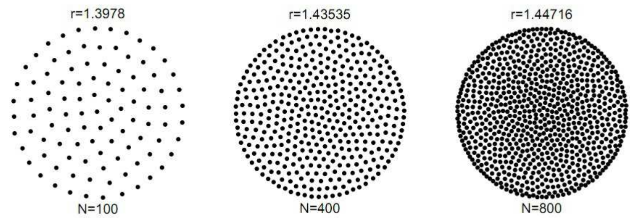

- If $GL^3 < 1$, the system is ***non-confining*** (or h-stable): doubling N doubles the cloud volume but density is unchanged:

$$G = 0.5, \quad L = 1.2$$

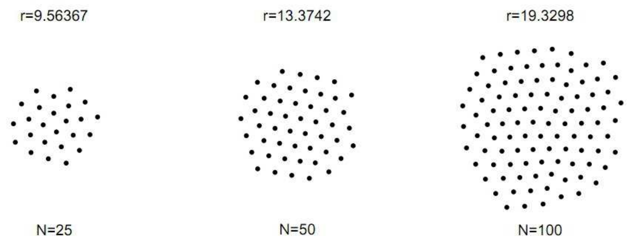

Continuum limit

- For confining potentials, we can take the continuum limit as the number of particles $N \to \infty$.

- We define the ***density*** ρ as

$$\int_D \rho(x)dx \approx \frac{\#\text{particles inside domain } D}{N}$$

- The flow is then characterized by density ρ and velocity field v:

$$\rho_t + \nabla \cdot (\rho v) = 0; \qquad v(x) = \int_{\mathbb{R}^n} F\left(|x-y|\right) \frac{x-y}{|x-y|} \rho(y)dy. \tag{3}$$

- Variational formulation: Let

$$E\left[\rho\right] := \int_{\mathbb{R}^n} \int_{\mathbb{R}^n} \rho(x)\rho(y)P(|x-y|)dxdy; \quad P'(r) = -F(r) \tag{4}$$

  Then (3) is the gradient flow of E; minima of E are stable equilibria of (3).

- Questions

  1. Describe the equilibrium cloud shape in the limit $t \to \infty$
  2. What about dynamics?

Turing analysis in 1D:

$$\rho_t + \nabla \cdot (v\rho) = 0; \qquad v = K * \rho, \quad K(x) = F(|x|)\,\mathrm{sign}(x). \tag{5}$$

- Note that $K * 1 = 0$ (since kernel K is odd) so that $\rho \equiv 1$ is a steady state.
- Linearize around homogeneous state $\rho = 1$:

$$\rho(x,t) = 1 + \phi(x,t), \quad \phi \ll 1$$

$$\phi_t + (K * \phi)_x = 0$$

- Plug in $\phi = e^{\lambda t} e^{imx}$:

$$\begin{aligned} K * \exp(imx) &= \int_{-\infty}^{\infty} F(|y|)\,\mathrm{sign}(y)\exp(imx - imy)dy \\ &= \exp(imx)\int_{-\infty}^{\infty} \underbrace{F(|y|)\,\mathrm{sign}(y)}_{odd}\left\{\underbrace{\cos(imy)}_{even} - i\,\underbrace{\sin(imy)}_{odd}\right\}dy \\ &= -2i\exp(imx)\int_0^{\infty} F(y)\sin(my)dy \end{aligned}$$

$$\boxed{\lambda = -2m\int_0^{\infty} F(y)\sin(my)dy}$$

- ***Conclusion: The homogeneous state is stable if and only if*** $\int_0^\infty F(y)\sin(my)dy > 0$ ***for all*** $m > 0$.

- In particular, ***patterns form*** (w.r.t. low frequencies) if $\int_0^\infty F(y)ydy < 0$.

- ***Patterns form when the constant state is unstable!***

- In the case of the repulsive-attractive morse potential:

$$F(r) = \exp(-r) - G\exp(-r/L); \;\; G < 1, L > 1$$

$$\lambda(m) = -2m^2\left(\frac{1}{m^2+1} - \frac{G}{m^2 + \left(\frac{1}{L}\right)^2}\right)$$

$$\lambda(0) = -2(1 - GL^2)$$

- Conclusions:
  - Homogenous state is unstable iff $GL^2 > 1$
  - Confining potential [i.e. "catostrophic case" iff $GL^2 > 1$].

Turing in any dimension d

- Exercise: In dimension d, homogeneous state is unstable (wrt small m) when $\int_0^\infty F(r) r^d dr < 0$.

- For Morse force, confining potential if $GL^{d+1} > 1$.

Complex patterns:

$$F(r) = \tanh\left((1-r)a\right) + b; \quad 0 < a; \;\; -1 < b < 1.$$

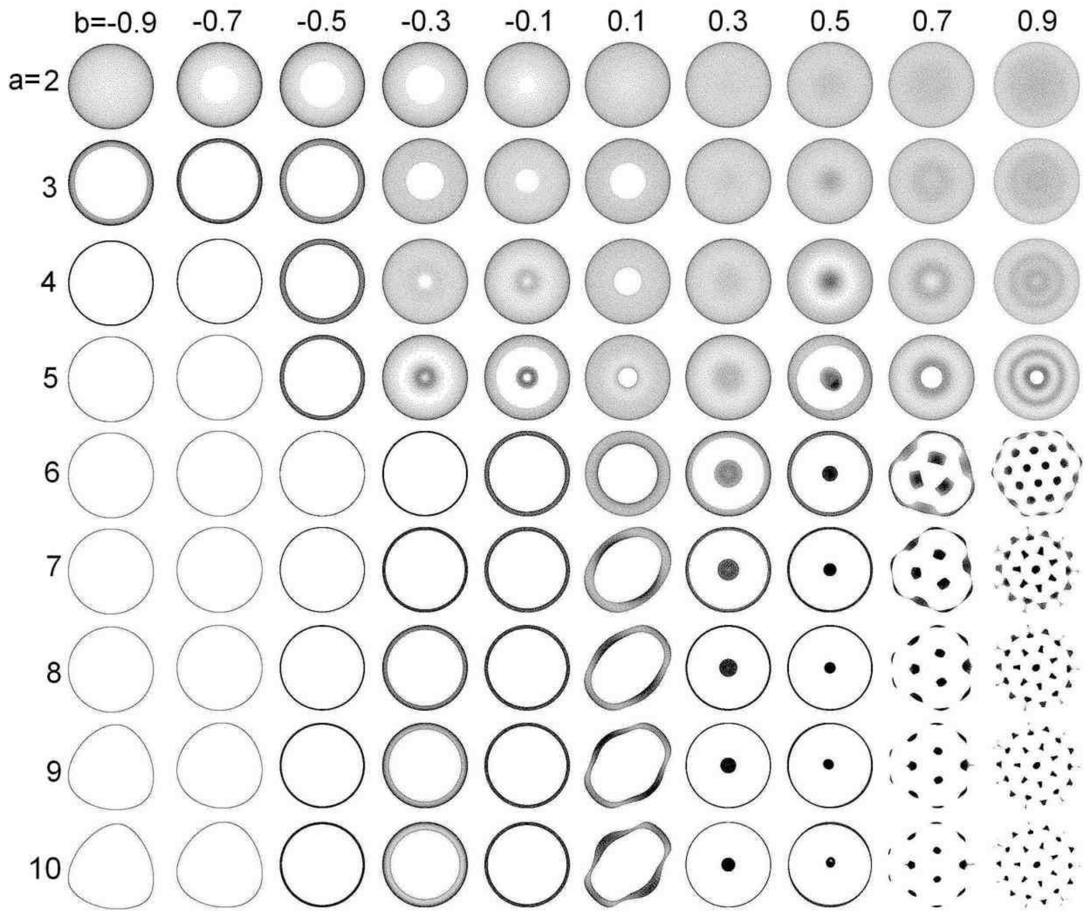

PW-linear force: $F(r) = \min(ar + b, 1 - r)$

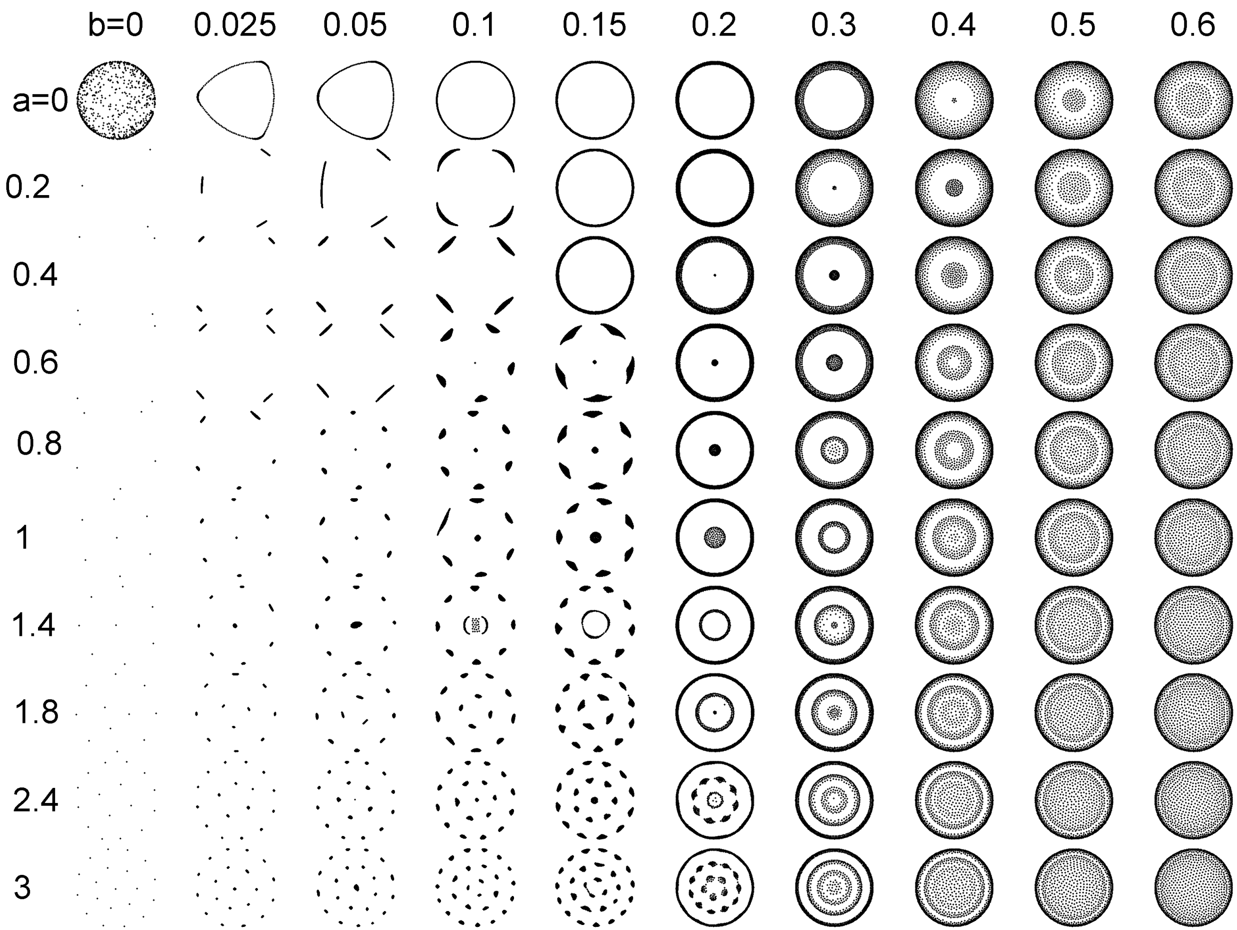

Ring-type steady states

- Seek steady state of the form $x_j = r\left(\cos\left(2\pi j/N\right), \sin\left(2\pi j/N\right)\right),\ j = 1\ldots N.$

- In the limit $N \to \infty$ **the radius of the ring must be the root of**

$$I(r) := \int_0^{\frac{\pi}{2}} F(2r\sin\theta)\sin\theta d\theta = 0. \tag{6}$$

- For Morse force $F(r) = \exp(-r) - G\exp(-r/L)$, such root exists whenever $GL^2 > 1$ [coincides with 1D catastrophic regime]

- For general repulsive-attractive force $F(r)$, a ring steady state exists if $F(r) \leq C < 0$ for all large r.

- Even if the ring steady-state exists, the time-dependent problem can be ill-posed!

Continuum limit for curve solutions

- If particles concentrate on a curve, in the limit $N \to \infty$ we obtain

$$\rho_t = \rho \frac{< z_\alpha, z_{\alpha t} >}{|z_\alpha|^2}; \quad z_t = K * \rho \tag{7}$$

where $z(\alpha; t)$ is a parametrization of the solution curve; $\rho(\alpha; t)$ is its density and

$$K * \rho = \int F(|z(\alpha') - z(\alpha)|) \frac{z(\alpha') - z(\alpha)}{|z(\alpha') - z(\alpha)|} \rho(\alpha', t) dS(\alpha'). \tag{8}$$

- Depending on $F(r)$ and initial conditions, the curve evolution may be ***ill-defined!***
  - For example a circle can degenerate into an annulus, gaining a dimension.
- We used a Lagrange particle-based numerical method to resolve (7).
  - Agrees with direct simulation of the ODE system (1):

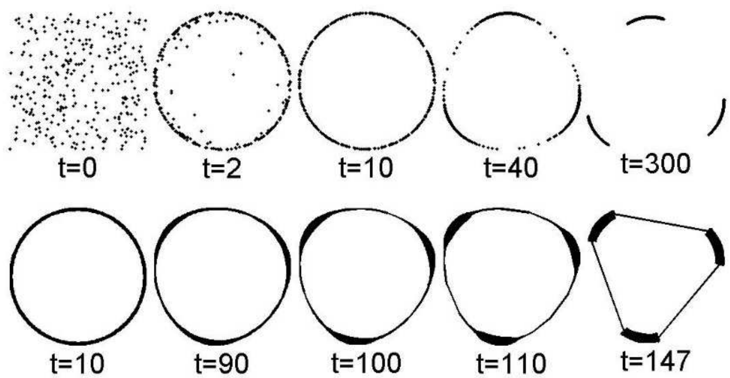

Local stability of a ring

- Turing-type analysis (linearization around the ring solution)

- Direct approach for ODE linearization:

$$x_k = r_0 \exp\left(2\pi i k/N\right)\left(1+\exp(t\lambda)\phi_k\right), \quad \phi_k \ll 1.$$

- After some algebra:

$$\begin{aligned}\lambda\phi_j = \frac{1}{N}\sum_{k\neq j} & G_+\left(\tfrac{\pi(k-j)}{N}\right)\left(\phi_j - \phi_k \exp\left(\tfrac{2\pi i(k-j)}{N}\right)\right)\\ & + G_-\left(\tfrac{\pi(k-j)}{N}\right)\left(\bar\phi_k - \bar\phi_j \exp\left(\tfrac{2\pi i(k-j)}{N}\right)\right),\end{aligned}$$

$$G_+ = \frac{1}{2}F'(2r_0\left|\sin\theta\right|) + \frac{F(2r_0\left|\sin\theta\right|)}{4r_0\left|\sin\theta\right|}; \quad G_- = \frac{1}{2}F'(2r_0\left|\sin\theta\right|) - \frac{F(2r_0\left|\sin\theta\right|)}{4r_0\left|\sin\theta\right|}.$$

- Anzatz:

$$\phi_j = b_+ e^{2m\pi i j/N} + b_- e^{-2m\pi i j/N}$$

$$\lambda \begin{pmatrix} b_+ \\ b_- \end{pmatrix} = M(m) \begin{pmatrix} b_+ \\ b_- \end{pmatrix}, \qquad M(m) := \begin{bmatrix} I_1(m) & I_2(m) \\ I_2(m) & I_1(-m) \end{bmatrix}; \;\; m = 1, 2, \ldots; \tag{9}$$

$$I_1(m) = \frac{4}{N} \sum_{l=1}^{N/2} G_+ \left(\frac{\pi l}{N}\right) \sin^2 \left((m+1)\frac{\pi l}{N}\right);$$

$$I_2(m) = \frac{4}{N} \sum_{l=1}^{N/2} G_- \left(\frac{\pi l}{N}\right) \left[\sin^2 \left(\frac{\pi l}{N}\right) - \sin^2 \left(m\frac{\pi l}{N}\right)\right].$$

- Taking the limit $N \to \infty$, we obtain

$$I_1(m) = \frac{2}{\pi} \int_0^{\frac{\pi}{2}} \left[\frac{F(2r\sin\theta)}{2r\sin\theta} + F'(2r\sin\theta)\right] \sin^2((m+1)\theta)\, d\theta; \tag{10a}$$

$$I_2(m) = \frac{2}{\pi} \int_0^{\frac{\pi}{2}} \left[\frac{F(2r\sin\theta)}{2r\sin\theta} - F'(2r\sin\theta)\right] \left[\sin^2(m\theta) - \sin^2(\theta)\right] d\theta. \tag{10b}$$

- Eigenfunction is a pure fourier mode when projected to the curvilinear coordinates of the circle.

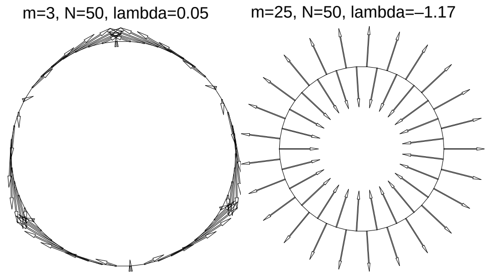

Quadratic force $F(r) = r - r^2$

- Computing explicitly,

$$\text{tr}\, M(m) = -\frac{\left(4m^4 - m^2 - 9\right)}{(4m^2-1)(4m^2-9)} < 0, \quad m = 2, 3, \ldots$$
$$\det M(m) = \frac{3m^2(2m^2+1)}{(4m^2-9)(4m^2-1)^2} > 0, \quad m = 2, 3, \ldots$$

- Conclusion: **ring pattern corresponding to $F(r) = r - r^2$ is locally stable**

- For large m, the two eigenvalues are $\lambda \sim -\frac{1}{4}$ and $\lambda \sim -\frac{3}{8m^2} \to 0$ as $m \to \infty$. The presence of arbitrary small eigenvalues implies the existence of very slow dynamics near the ring equilibrium.

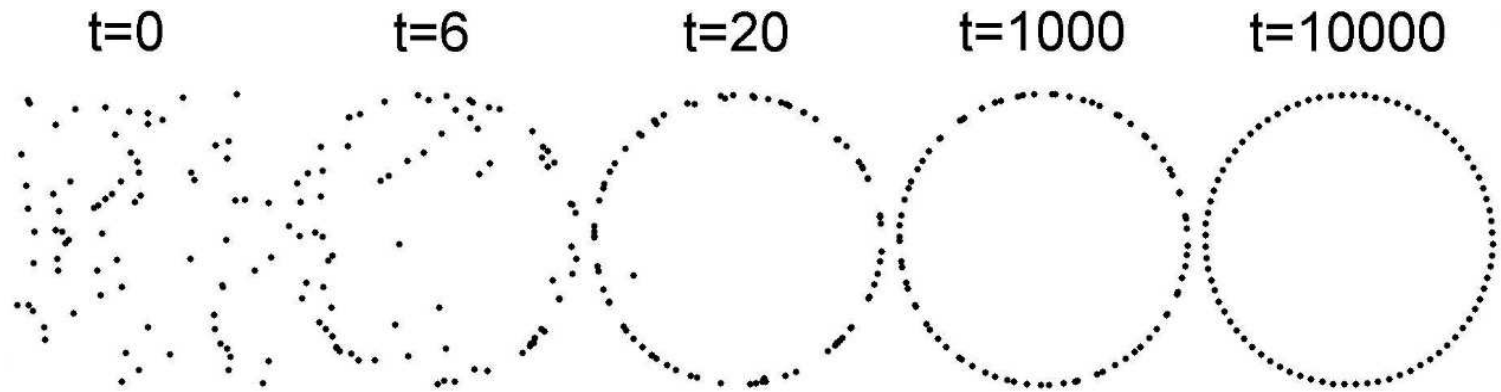

General power force

$$F(r) = r^p - r^q, \;\; 0 < p < q$$

- The mode $m = \infty$ is stable if and only if $pq > 1$ and $p < 1$.
- Stability of other modes can be expressed in terms of Gamma functions.
- The dominant unstable mode corresponds to $m = 3$; the boundary is given by
$$0 = 723 - 594(p+q) - 27(p^2+q^2) - 431pq + 106\left(pq^2+p^2q\right) + 19\left(p^3q+pq^3\right)$$
$$+ 10\left(p^3q^2+p^2q^3\right) + 6\left(p^3+q^3\right) + p^3q^3;$$
- Boundaries for $m = 4, 5, \ldots$ are similarly expressed in terms of higher order polynomials in p, q.

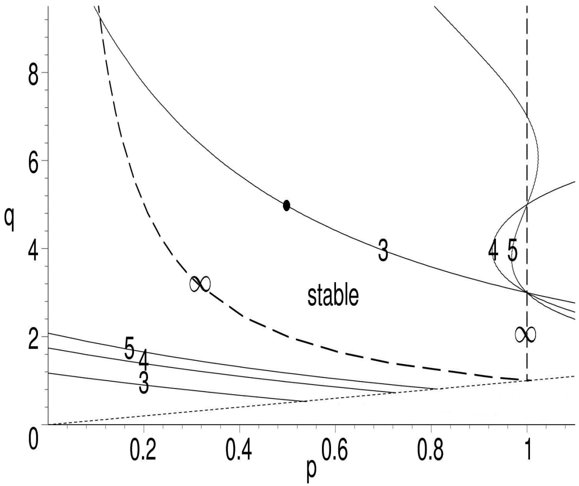

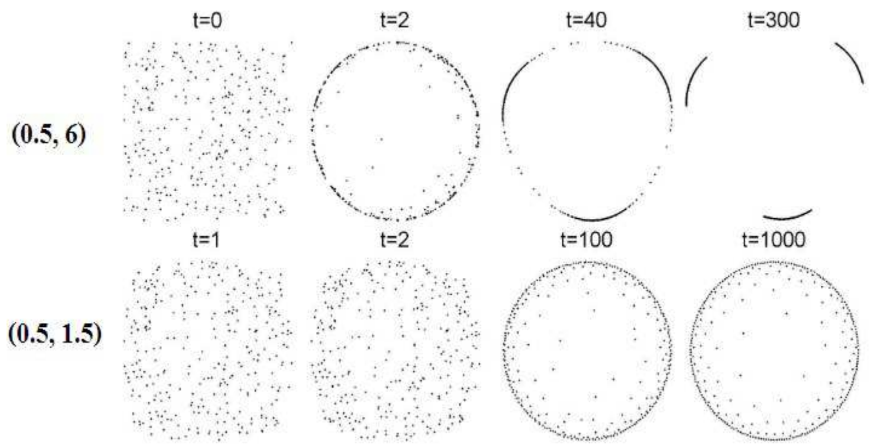

Weakly nonlinear analysis

- Near the instability threshold, higher-order analysis shows a **supercritical pitchfork bifurcation,** whereby a ring solution bifurcates into an $m-$symmetry breaking solution
- This shows existence of nonlocal solutions.
- Example: $F(r) = r^{1.5} - r^q$; bifurcation $m = 3$ occurs at $q = q_c \approx 4.9696$; nonlinear analysis predicts

$$\max_i |x_i| - \min_i |x_i| = \sqrt{\max(0, \tau(q - q_c))}; \quad \tau \approx 0.109.$$

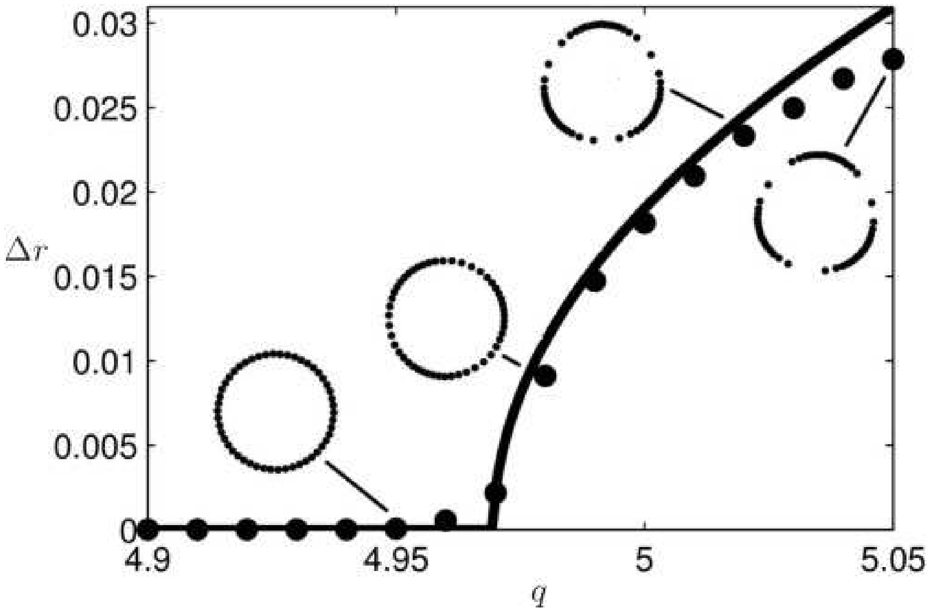

Point-concentration (hole) solutions

$$F(r) = \min(ar, r - r^2)$$

Solutions consist of K “clusters”, where each cluster has N/K points inside. The number K depends on a :

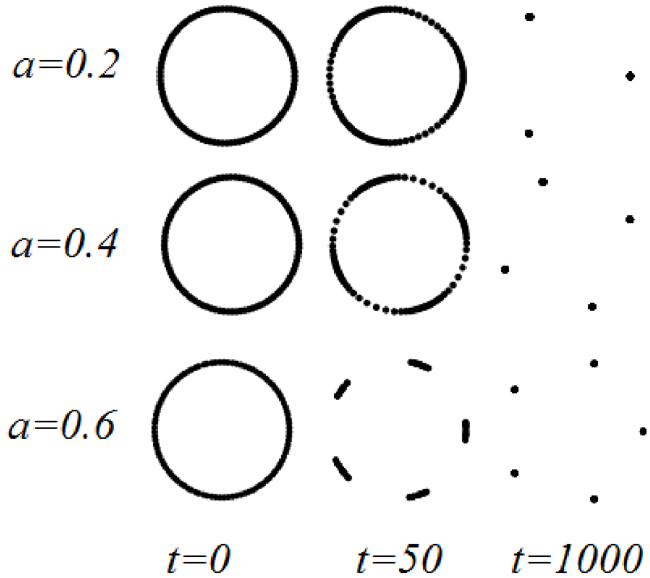

Spots: "degenerate" holes

$$F(r) = \min(ar + \delta, 1 - r); \quad \delta \ll 1$$

- Points degenerate into spots of size $O(\delta)$. eg. $a = 0.3, \delta = 0.05$:

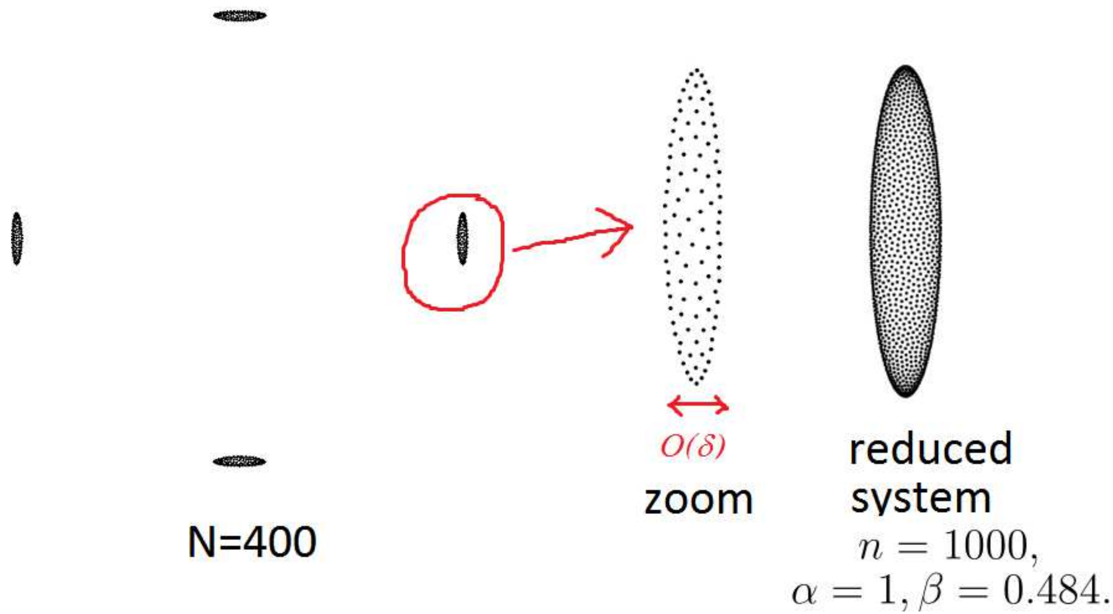

- Inside each of the cluster, the ***reduced*** problem is:

$$\phi_l' = \sum_{j \neq l}^{n} \frac{\phi_l - \phi_j}{|\phi_l - \phi_j|} - n \begin{bmatrix} \alpha & 0 \\ 0 & \beta \end{bmatrix} \phi_l$$

- α, β depend only on $F(r)$ not on N.

(In)stability of $m \gg 1$ modes

- If $\lambda(m) > 0$ for all sufficiently large m, then we call the ring solution **ill-posed.** Otherwise we call it **well-posed**.

- For ill-posed problems, the ring can degenerate into either an annulus (eg. $F(x) = 0.5 + x - x^2$) or discrete set of points (eg $F(x) = x^{1.3} - x^2$)

- , **if** $F(r)$ **is** C^4 on $[0, 2r]$**, then the necessary and sufficient conditions for well-posedness of a ring are:**

$$F(0) = 0, \quad F''(0) < 0 \text{ and} \tag{11}$$

$$\int_0^{\pi/2} \left(\frac{F(2r\sin\theta)}{2r\sin\theta} - F'(2r\sin\theta) \right) d\theta < 0. \tag{12}$$

- Ring solution for the morse force $F(r) = \exp(-r) - G\exp(-r/L)$ is always ill-posed since $F(0) > 0$.

Bifurcation to annulus:

Consider

$$F(r) = r - r^2 + \delta, \qquad 0 \le \delta \ll 1.$$

- A ring is stable of radius $R \sim \frac{3\pi}{16} + \frac{2}{\pi}\delta + O(\delta^2)$ if $\delta = 0$ but ***high modes*** become unstable for $\delta > 0$

- The most unstable mode in the ***discrete*** system is $m = N/2$ and can be stable even if the continuous model is ill-posed!

- **Proposition: Let**

$$N_c \sim \frac{\pi}{4} e^{4-\gamma} \exp\left(\frac{3\pi^2}{64\delta}\right).$$

  The ring is stable if $N < N_c$.

- For $N > N_c$ but $N \sim N_c$, solution consists of two radii $R \pm \varepsilon$ where

$$R = \frac{3\pi}{32}\left(1 + \sqrt{1 + \frac{128}{3\pi^2}\delta}\right); \quad \varepsilon \sim 4Re^{-2} \exp\left(\frac{-4R^2 + R\pi/2}{\delta}\right)$$

- Example: $\delta = 0.35 \implies N_c \sim 90,\ 2\varepsilon \sim 0.033$. Numerically, we obtain $2\varepsilon \approx 0.036$. Good agreement!

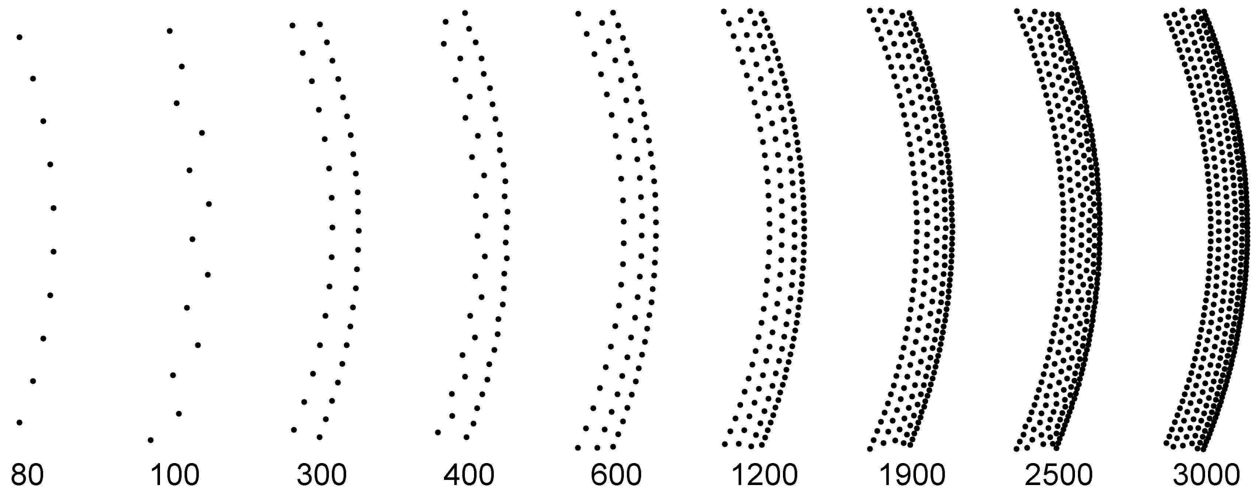

- Increasing N further, more rings appear until we get a thin annulus of width $O(\varepsilon)$.

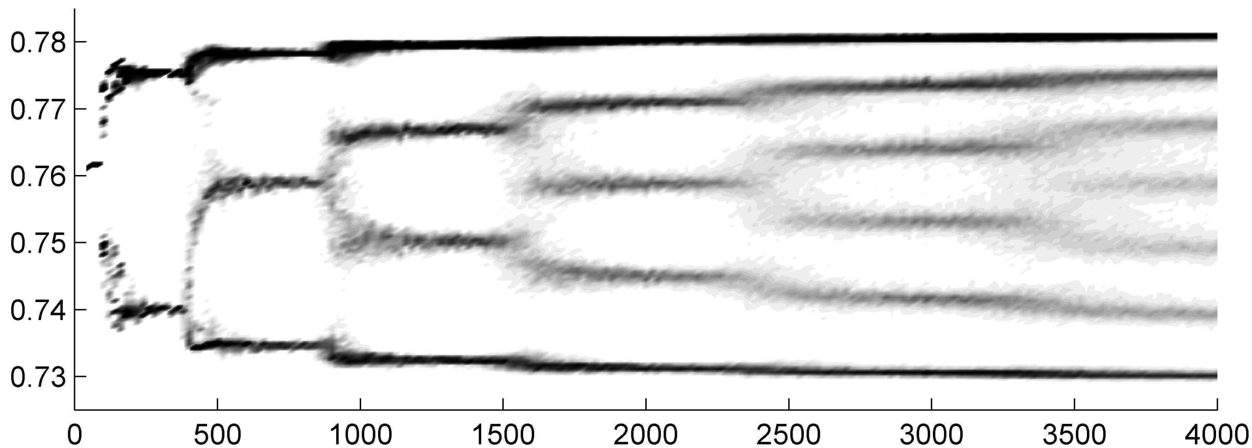

Annulus: continuum limit $N \gg N_c$:

- $F(r) = r - r^2 + \delta, \qquad 0 < \delta \ll 1$
- **Main result:** In the limit $\delta \to 0$, the annulus inner and outer radii R_1, R_2 are given by

$$R \sim \frac{3\pi}{16} + \frac{2}{\pi}\delta; \qquad R_1 \sim R - \beta, \quad R_2 \sim R + \beta$$

  where

$$\beta \sim 3\pi e^{-5} \exp\left(-\frac{3\pi^2}{64}\frac{1}{\delta}\right) \ll \delta \ll 1.$$

  The radial density profile inside the annulus is

$$\rho(x) \sim \begin{cases} \dfrac{c}{\sqrt{\beta^2 - (R - |x|)^2}}, & |R - x| < \beta \ll 1 \\ 0, & \text{otherwise} \end{cases}$$

- Annulus is ***exponentially thin in*** δ... note the 1/sqrt singularity near the edges!

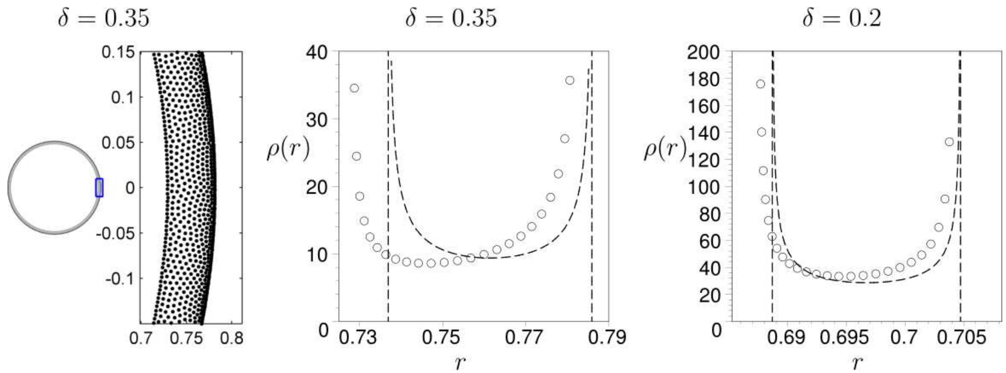

Key steps for computing annulus profile

- For radially symmetric density, the velocity field reduces to a 1D problem:

$$v(r) = \int_0^\infty K(s,r)\rho(s)sds$$

where

$$K(s,r) := \int_0^{2\pi} (r - s\cos\theta)\, f\left(\sqrt{r^2 + s^2 - 2rs\cos\theta}\right) d\theta; \quad f(r) = 1 - r + \frac{\delta}{r}$$

- Assume thin annulus; expand all integrals. ***It boils down to*** integral equation

$$\int_{-\beta}^{\beta} \ln|\eta - \xi|\, \varrho(\eta)d\eta = 1 \text{ for all } \xi \in (\alpha, \beta)$$

- ***Explicit solution*** is a special case of Formula 3.4.2 from “Handbook of integral equations” A.Polyanin and A.Manzhirov:

$$\varrho(\xi) = \frac{C}{\sqrt{\beta^2 - \xi^2}}$$

3D sphere instabilities

- Radius satisfies: $\int_0^{\pi} F(2r_0 \sin\theta)\sin\theta \sin 2\theta = 0$

- Instability can be done using spherical harmonics

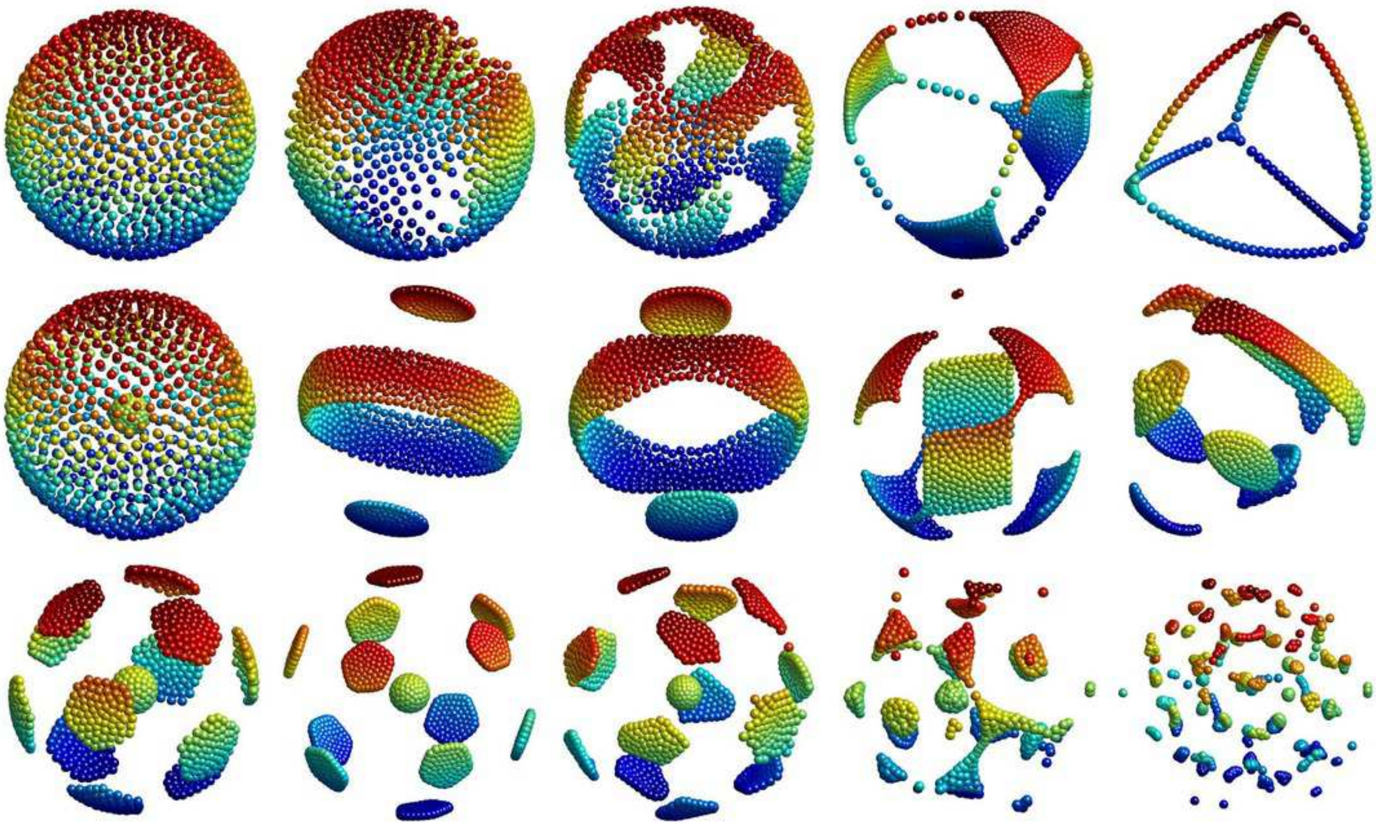

Stability of a spherical shell

Define

$$g(s) := \frac{F(\sqrt{2s})}{\sqrt{2s}};$$

The spherical shell has a radius given implicitly by

$$0 = \int_{-1}^{1} g(R^2(1-s))(1-s)\mathrm{d}s.$$

Its stability is given by a sequence of 2x2 eigenvalue problems

$$\lambda \begin{pmatrix} c_1 \\ c_2 \end{pmatrix} = \begin{pmatrix} \alpha + \lambda_l(g_1) & l(l+1)\lambda_l(g_2) \\ \lambda_l(g_2) & \frac{l(l+1)}{R^2}\lambda_l(g_3) \end{pmatrix} \begin{pmatrix} c_1 \\ c_2 \end{pmatrix}, \qquad l = 2, 3, 4, \ldots$$

where

$$\lambda_l(f) := 2\pi \int_{-1}^{1} f(s)P_l(s)\, \mathrm{d}s;$$

with $P_l(s)$ the Legendre polynomial and

$$\alpha := 8\pi g(2R^2) + \lambda_0(g(R^2(1-s^2)))$$

$$g_1(s) := R^2 g'(R^2(1-s))(1-s)^2 - g(R^2(1-s))s$$

$$g_2(s) := g(R^2(1-s))(1-s); \qquad g_3(s) := \int_0^{R^2(1-s)} g(z)dz.$$

Well-posedness in 3D

Suppose that $g(s)$ can be written in terms of the generalized power series as

$$g(s) = \sum_{i=1}^{\infty} c_i s^{p_i}, \quad p_1 < p_2 < \cdots \quad \text{with} \quad c_1 > 0.$$

Then the ring is **well-posed** [i.e. $\lambda < 0$ for all sufficiently large l] if

$$\text{(i)} \;\; \alpha < 0 \quad \text{and} \quad \text{(ii)} \;\; p_1 \in (-1,0) \bigcup (1,2) \bigcup (3,4) \ldots$$

The ring is **ill-posed [**i.e. $\lambda > 0$ for all sufficiently large l] if either $\alpha > 0$ or $p_1 \notin [-1,0] \bigcup [1,2] \bigcup [3,4] \ldots$

Key identity to prove well-posedness:

$$\int_{-1}^{1} (1-s)^p P_l(s)\,\mathrm{d}s = \frac{2^{p+1}}{p+1}\frac{\Gamma(l-p)\Gamma(p+2)}{\Gamma(l+p+2)\Gamma(-p)}$$
$$\sim -\frac{1}{\pi}\sin(\pi p)\,\Gamma^2(p+1)2^{p+1}l^{-2p-2} \quad \text{as } l \to \infty.$$

Proof:

- Use hypergeometric representation: $P_l(s) = {}_2F_1\left(\begin{matrix} l+1, -l \\ 1 \end{matrix}; \frac{1-s}{2}\right)$.

- Use **generalized Euler transform**:

$${}_{A+1}F_{B+1}\left(\begin{matrix} a_1,\ldots,a_A,c \\ b_1,\ldots,b_B,d \end{matrix}; z\right) = \frac{\Gamma(d)}{\Gamma(c)\Gamma(d-c)}\int_0^1 t^{c-1}(1-t)^{d-c-1}{}_AF_B\left(\begin{matrix} a_1,\ldots,a_A, c \\ b_1,\ldots,b_B, d \end{matrix}\right.$$

to get $\int_{-1}^{1}(1-s)^p P_l(s)\,\mathrm{d}s = \frac{2\pi 2^{p+1}}{p+1}{}_3F_2\left(\begin{matrix} p+1, l+1, -l \\ p+2, 1 \end{matrix}; 1\right)$.

- Apply the **Saalschütz Theorem** to simplify

$${}_3F_2\left(\begin{matrix} p+1, l+1, -l \\ p+2, 1 \end{matrix}; 1\right) = \frac{\Gamma(l-p)\Gamma(p+2)}{\Gamma(l+p+2)\Gamma(-p)}.$$

Generalized Lennard-Jones interaction

$$g(s) = s^{-p} - s^{-q}; \qquad 0 < p, q < 1; \;\; p > q$$

- Well posed if $q < \frac{2p-1}{2p-2}$; ill-posed if $q > \frac{2p-1}{2p-2}$.

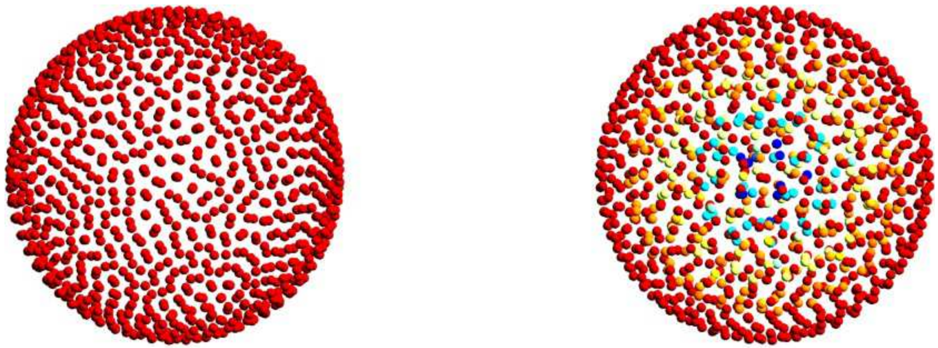

(a) (b)

Example: steady state with $N = 1000$ particles. (a) $(p, q) = (1/3, 1/6)$. Particles concentrate uniformly on a surface of the sphere, with no particles in the interior. (b) $(p, q) = (1/2, 1/4)$. Particles fill the interior of a ball. The particles are color-coded according to their distance from the center of mass.

Custom-designed kernels

- In 3D, we can design force $F(r)$ which is stable for all modes except specified mode.
- EXAMPLE: Suppose we want only mode $m = 5$ to be unstable. Using our algorithm, we get

$$F(r) = \left\{ 3\left(1 - \frac{r^2}{2}\right)^2 + 4\left(1 - \frac{r^2}{2}\right)^3 - \left(1 - \frac{r^2}{2}\right)^4 \right\} r + \varepsilon; \quad \varepsilon = 0.1.$$

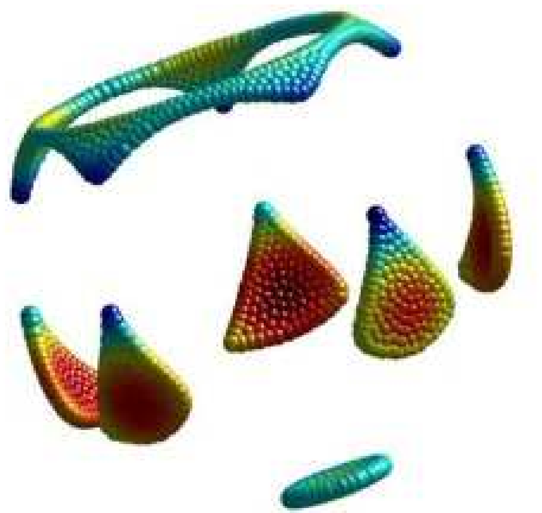

Particle simulation

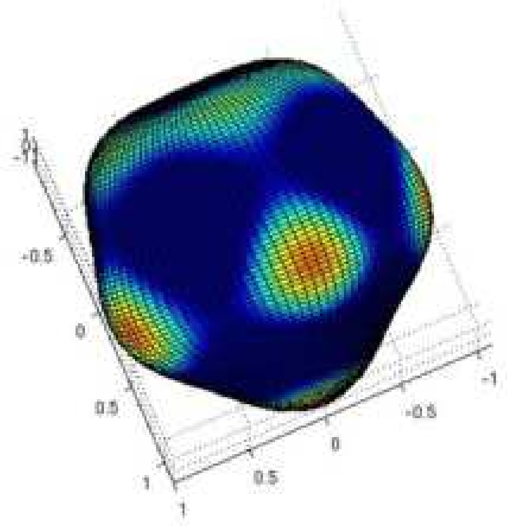

Linearized solution

Part II: Constant-density swarms

- Biological swarms have sharp boundaries, relatively **constant internal population.**
- Question: ***What interaction force leads to such swarms?***
- More generally, can we deduce an interaction force from the swarm density?

Bounded states of constant density

Claim. Suppose that

$$\boxed{F(r) = \frac{1}{r^{n-1}} - r, \quad \text{where } n \equiv \text{dimension}}$$

Then the aggregation model

$$\rho_t + \nabla \cdot (\rho v) = 0; \qquad v(x) = \int_{\mathbb{R}^n} F\left(|x-y|\right) \frac{x-y}{|x-y|} \rho(y) dy.$$

admits a steady state of the form

$$\rho(x) = \begin{cases} 1, & |x| < R \\ 0, & |x| > R \end{cases}; \quad v(x) = \begin{cases} 0, & |x| < 1 \\ -ax, & |x| > 1 \end{cases}.$$

where $R = 1$ for $n = 1, 2$ and $a = 2$ in one dimension and $a = 2\pi$ in two dimensions.

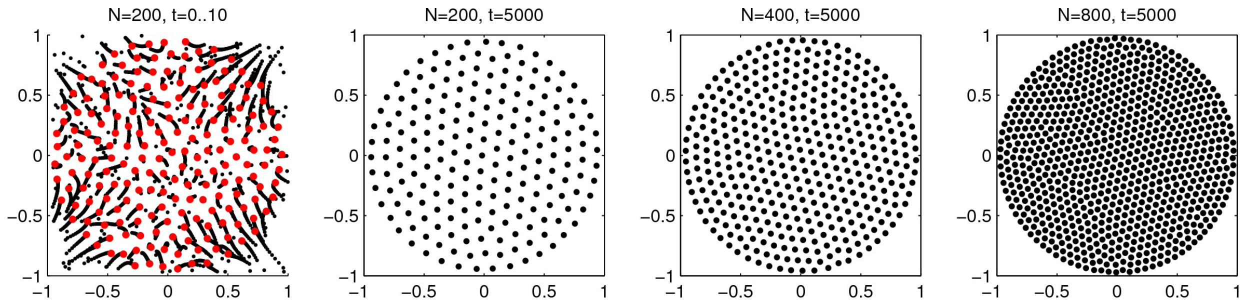

Proof for two dimensions

Define

$$G(x) := \ln|x| - \frac{|x|^2}{2}; \quad M = \int_{\mathbb{R}^n} \rho(y)dy$$

Then we have:

$$\nabla G = F(|x|)\frac{x}{|x|} \quad \text{and} \quad \Delta G(x) = 2\pi\delta(x) - 2.$$

so that

$$v(x) = \int_{\mathbb{R}^n} \nabla_x G(x-y)\rho(y)dy.$$

Thus we get:

$$\begin{aligned}
\nabla \cdot v &= \int_{\mathbb{R}^n} (2\pi\delta(x-y) - 2)\rho(y)dy \\
&= 2\pi\rho(x) - 2M \\
&= \begin{cases} 0, & |x| < R \\ -2M, & |x| > R \end{cases}
\end{aligned}$$

The steady state satisfies $\nabla \cdot v = 0$ inside some ball of radius R with $\rho = 0$ outside such a ball but then $\rho = M/\pi$ inside this ball and $M = \int_{\mathbb{R}^n} \rho(y)dy = MR^2 \implies R = 1$.

Dynamics in 1D with $F(r) = 1 - r$

Assume WLOG that

$$\int_{-\infty}^{\infty} x\rho(x) = 0; \quad M := \int_{-\infty}^{\infty} \rho(x)\,dx$$

Then

$$\begin{aligned} v(x) &= \int_{-\infty}^{\infty} F\left(|x-y|\right) \frac{x-y}{|x-y|}\rho(y)dy \\ &= \int_{-\infty}^{\infty} \left(1 - |x-y|\right) \operatorname{sign}(x-y)\rho(y) \\ &= 2\int_{-\infty}^{x} \rho(y)dy - M(x+1). \end{aligned}$$

and continuity equations become

$$\begin{aligned} \rho_t + v\rho_x &= -v_x\rho \\ &= \left(M - 2\rho\right)\rho \end{aligned}$$

Define the characteristic curves $X(t, x_0)$ by

$$\frac{d}{dt}X(t; x_0) = v; \qquad X(0, x_0) = x_0$$

Then along the characteristics, we have $\rho = \rho(X, t)$;

$$\frac{d}{dt}\rho = \rho(M - 2\rho)$$

Solving we get:

$$\rho(X(t, x_0), t) = \frac{M}{2 + e^{-Mt}(M/\rho_0 - 2)}; \qquad \rho(X(t, x_0), t) \to M/2 \text{ as } t \to \infty$$

Solving for characteristic curves

Let

$$w := \int_{-\infty}^{x} \rho(y)dy$$

then

$$v = 2w - M(x+1); \quad v_x = 2\rho - M$$

and integrating $\rho_t + (\rho v)_x = 0$ we get:

$$w_t + vw_x = 0$$

Thus w is constant along the characteristics X of ρ, so that characteristics $\frac{d}{dt}X = v$ become

$$\frac{d}{dt}X = 2w_0 - M(X+1); \quad X(0; x_0) = x_0$$

Summary for $F(r) = 1 - r$ in 1D:

$$X = \frac{2w_0(x_0)}{M} - 1 + e^{-Mt}\left(x_0 + 1 - \frac{2w_0(x_0)}{M}\right)$$

$$w_0(x_0) = \int_{-\infty}^{x_0} \rho_0(z)dz; \quad M = \int_{-\infty}^{\infty} \rho_0(z)dz$$

$$\rho(X,t) = \frac{M}{2 + e^{-tM}(M/\rho_0(x_0) - 2)}$$

Example: $\rho_0(x) = \exp\left(-x^2\right)/\sqrt{\pi}; \quad M = 1:$

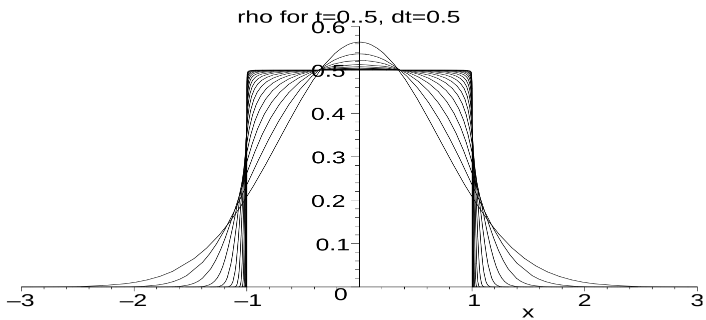

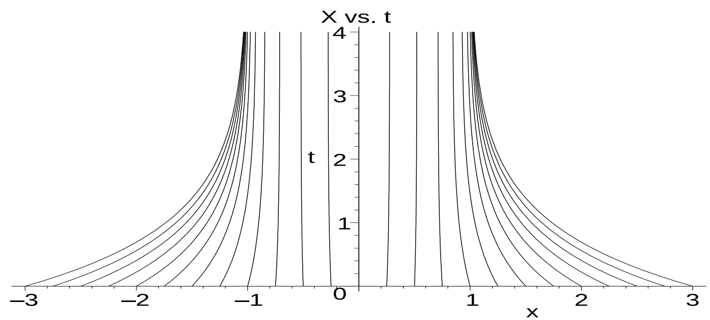

Global stability

In limit $t \to \infty$ we get:

$$X = \frac{2w_0}{M} - 1; \quad w_0 = 0 \ldots M; \quad \rho(X, \infty) = \frac{M}{2}$$

We have shown that as $t \to \infty$, the steady state is

$$\rho(x, \infty) = \begin{cases} M/2, & |x| < 1 \\ 0, & |x| > 1 \end{cases} \tag{13}$$

- This **proves the global stability of (13)!**

- Characteristics intersect at $t = \infty$; solution forms a shock at $x = \pm 1$ at $t = \infty$.

Dynamics in 2D, $F(r) = \frac{1}{r} - r$

- Similar to 1D,

$$\nabla \cdot v = 2\pi\rho(x) - 4\pi M;$$

$$\begin{aligned} \rho_t + v \cdot \nabla\rho &= -\rho\nabla \cdot v \\ &= -\rho\left(\rho - 2M\right)2\pi \end{aligned}$$

- Along the characterisitics:

$$\frac{d}{dt}X(t;x_0) = v; \qquad X(0,x_0) = x_0$$

we still get

$$\frac{d}{dt}\rho = 2\pi\rho(2M - \rho);$$

$$\rho(X(t;x_0),t) = \frac{2M}{1 + \left(\frac{2M}{\rho(x_0)} - 1\right)\exp\left(-4\pi M t\right)} \tag{14}$$

- Continuity equations yield:

$$\rho(X(t;x_0),t)\det\nabla_{x_0}X(t;x_0) = \rho_0(x_0)$$

- Using (14) we get

$$\det \nabla_{x_0} X(t;x_0) = \frac{\rho_0(x_0)}{2M} + \left(1 - \frac{\rho_0(x_0)}{2M}\right) \exp\left(-4\pi M t\right).$$

- If ρ is **radially symmetric**, characteristics are also radially symmetric, i.e.

$$X(t;x_0) = \lambda\left(\left|x_0\right|, t\right) x_0$$

then

$$\det \nabla_{x_0} X(t;x_0) = \lambda(t;r)\left(\lambda(t;r) + \lambda_r(t;r) r\right), \quad r = |x_0|$$

so that

$$\lambda^2 + \lambda_r \lambda r = \frac{\rho_0(x_0)}{2M} + \left(1 - \frac{\rho_0(x_0)}{2M}\right) \exp\left(-4\pi M t\right)$$

$$\lambda^2 r^2 = \frac{1}{M} \int_0^r s \rho_0(s) ds + 2 \exp\left(-4\pi M t\right) \int_0^r s \left(1 - \frac{\rho\left(s\right)}{2M}\right) ds$$

So **characteristics are fully solvable**!!

- This proves **global stability in the space of radial initial conditions** $\rho_0(x) = \rho_0(|x|)$**.**

- More general global stability is still open.

The force $F(r) = \frac{1}{r} - r^{q-1}$ in 2D

- If $q = 2$, we have explicit ode and solution for characteristics.

- For other q, no explicit solution is available but we have **differential inequalities:**

  Define
  $$\rho_{\max} := \sup_x \rho(x,t); \quad R(t) := \text{ radius of support of } \rho(x,t)$$
  Then
  $$\begin{aligned} \frac{d\rho_{\max}}{dt} &\leq (aR^{q-2} - b\rho_{\max})\rho_{\max} \\ \frac{dR}{dt} &\leq c\sqrt{\rho_{\max}} - dR^{q-1}; \end{aligned}$$
  where a, b, c, d are some [known] positive constants.

- It follows that if $R(0)$ is sufficiently big, then $R(t), \rho_{\max}(t)$ remain bounded for all t. [using bounding box argument]

- **Theorem:** For $q \geq 2$, there exists a bounded steady state [uniqueness??]

Inverse problem: Custom-designer kernels: 1D

Theorem. In one dimension, conisder a radially symmetric density of the form

$$\rho(x) = \begin{cases} b_0 + b_2 x^2 + b_4 x^4 + \ldots + b_{2n} x^{2n}, & |x| < R \\ 0, & |x| \geq R \end{cases} \tag{15}$$

Define the following quantities,

$$m_{2q} := \int_0^R \rho(r) r^{2q} dr. \tag{16}$$

Then $\rho(r)$ is the steady state corresponding to the kernel

$$F(r) = 1 - a_0 r - \frac{a_2}{3} r^3 - \frac{a_4}{5} r^5 - \ldots - \frac{a_{2n}}{2n+1} r^{2n+1} \tag{17}$$

where the constants $a_0, a_2, \ldots, a_{2n},$ are computed from the constants $b_0,\ b_2, \ldots, b_{2n}$ by solving the following linear problem:

$$b_{2k} = \sum_{j=k}^{n} a_{2j} \begin{pmatrix} 2j \\ 2k \end{pmatrix} m_{2(j-k)}, \qquad k = 0 \ldots n. \tag{18}$$

Example: custom kernels 1D

Example 1: $\rho = 1 - x^2, \;\; R = 1$, then $F(r) = 1 - 9/5r + 1/2r^3$.

Example 2: $\rho = x^2, \;\; R = 1$, then $F(r) = 1 + 9/5r - r^3$.

Example 3: $\rho = 1/2 + x^2 - x^4, \;\; R = 1$; then $F(r) = 1 + \frac{209425}{336091}r - \frac{4150}{2527}r^3 + \frac{6}{19}r^5$.

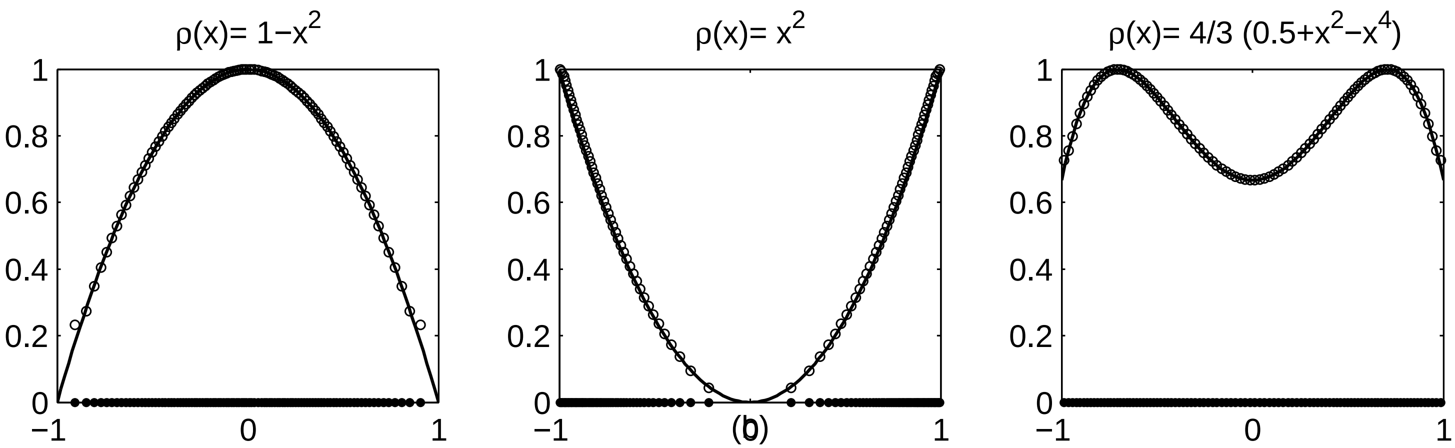

Ex.1 Ex.2 Ex.3

Inverse problem: Custom-designer kernels: 2D

Theorem. In **two dimensions**, conisder a radially symmetric density $\rho(x) = \rho(|x|)$ of the form

$$\rho(r) = \begin{cases} b_0 + b_2 r^2 + b_4 r^4 + \ldots + b_{2n} r^{2n}, & r < R \\ 0, & r \geq R \end{cases} \tag{19}$$

Define the following quantities,

$$m_{2q} := \int_0^R \rho(r) r^{2q} dr. \tag{20}$$

Then $\rho(r)$ is the steady state corresponding to the kernel

$$F(r) = \frac{1}{r} - \frac{a_0}{2} r - \frac{a_2}{4} r^3 - \ldots - \frac{a_{2n}}{2n+2} r^{2n+1} \tag{21}$$

where the constants $a_0, a_2, \ldots, a_{2n},$ are computed from the constants $b_0,\ b_2, \ldots, b_{2n}$ by solving the following linear problem:

$$b_{2k} = \sum_{j=k}^{n} a_{2j} \begin{pmatrix} j \\ k \end{pmatrix}^2 m_{2(j-k)+1}; \quad k = 0 \ldots n. \tag{22}$$

This system always has a unique solution for provided that $m_0 \neq 0$.

Numerical simulations, 1D

- First, use standard ODE solver to integrate the corresponding discrete particle model,

$$\frac{dx_j}{dt} = \frac{1}{N} \sum_{\substack{k=1\ldots N \\ k \neq j}} F\left(|x_j - x_k|\right) \frac{x_j - x_k}{|x_j - x_k|}, \quad j = 1 \ldots N.$$

- How to compute $\rho(x)$ from x_i? [Topaz-Bernoff, 2010]
  - Use x_i to approximate the cumulitive distribution, $w(x) = \int_{-\infty}^{x} \rho(z) dz$.
  - Next take derivative to get $\rho(x) = w'(x)$

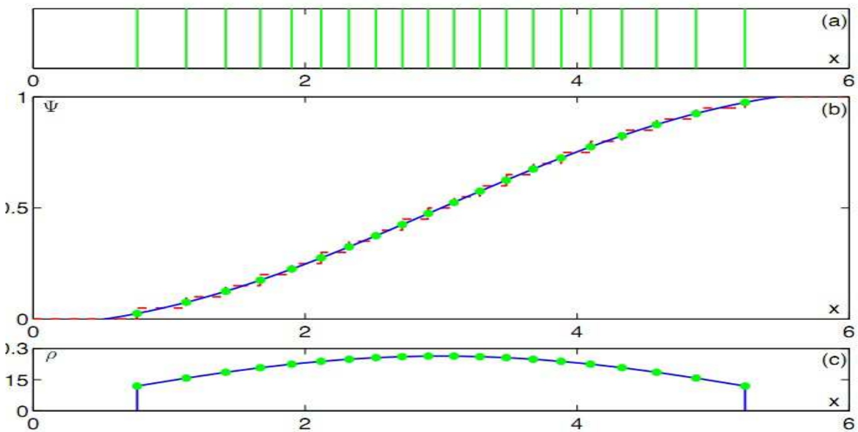

[Figure taken from Topaz+Bernoff, 2010 preprint]

Numerical simulations, 2D

- Solve for x_i using ODE particle model as before [$2N$ variables]
- Use x_i to compute **Voronoi diagram**;
- Estimate $\rho(x_j) = 1/a_j$ where a_j is the area of the voronoi cell around x_j.
- Use **Delanay triangulation** to generate smooth mesh.
- **Example:** Take

$$\rho(r) = \begin{cases} 1 + r^2, r < 1 \\ 0, \quad r > 0 \end{cases}$$

Then by Custom-designed kernel in 2D is:

$$F(r) = \frac{1}{r} - \frac{8}{27}r - \frac{r^3}{3}.$$

Running the particle method yeids...

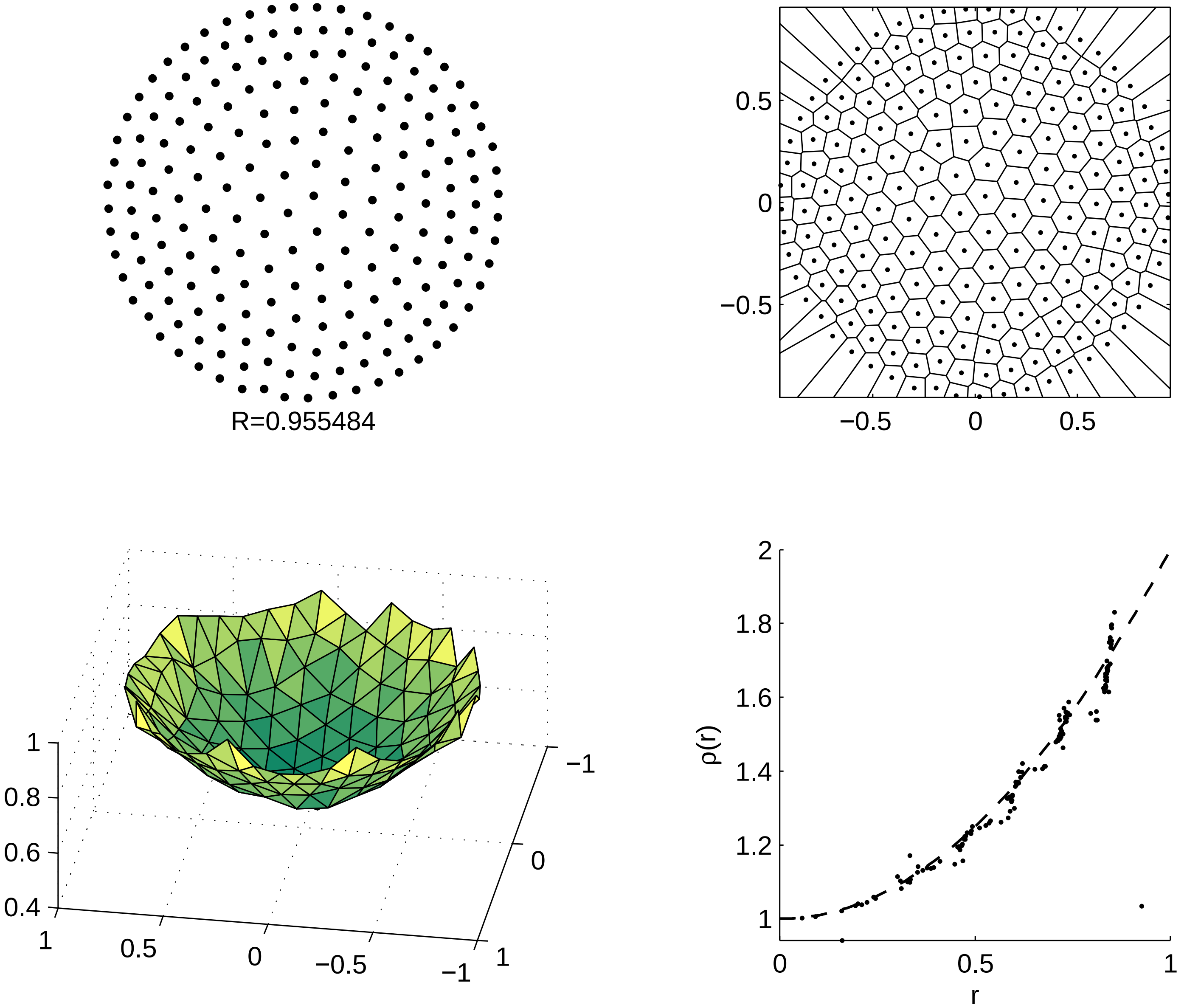

R=0.955484
0.5
0
−0.5
−0.5
0
0.5
1
0.8
0.6
0.4
1
0.5
0
−0.5
−1
−1
0
1
2
1.8
1.6
1.4
1.2
1
ρ(r)
0
0.5
1
r

Numerical solutions for radial steady states for $F(r) = \frac{1}{r} - r^{q-1}$

- Radial steady states of radius R satisfy $\rho(r) = 2q \int_0^R (r'\rho(r')I(r,r')dr'$

  where $c(q)$ is some constant and $I(r,r') = \int_0^\pi (r^2 + r'^2 - 2rr' \sin\theta)^{q/2-1} d\theta$.

- To find ρ and R, we adjust R until the operator $\rho \to c(q) \int_0^R (r'\rho(r')K(r,r')dr'$ has eigenvalue 1; then ρ is the corresponding eigenfunction.

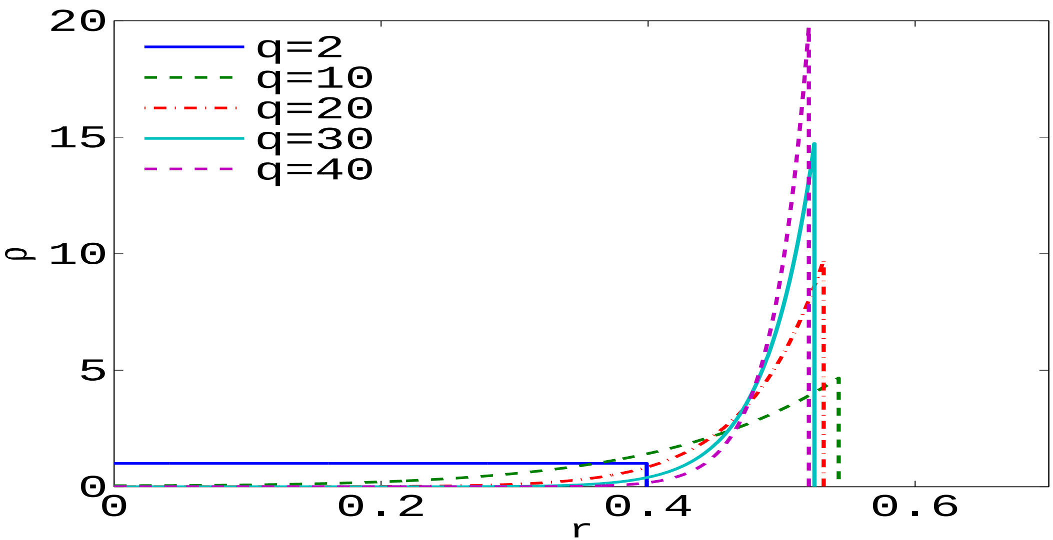

Vortex dynamics

- Equations first given by Helmholtz (1858): each vortex generates a rotational velocity field which advects all other vortices. ***Vortex model:***

$$\frac{dz_j}{dt} = i \sum_{k \neq j} \gamma_k \frac{z_j - z_k}{|z_j - z_k|^2}, \quad j = 1 \ldots N.$$

- Classical problem; observed in many physical experiments: floating magnetized needles (Meyer, 1876); Malmberg-Penning trap (Durkin & Fajans, 2000), Bose-Einstein Condensates (Ketterle et.al. 2001); magnetized rotating disks (Whitesides et.al, 2001)

- Conservative, hamiltonian system

- General initial conditions lead to chaos: $movie - chaos$

- Certain special configurations are "stable" in hamiltonial sense: $movie - stable$

- Rigidly rotating steady states are called ***relative equilibria***:

$$z_j(t) = e^{\omega i t} \xi_j \quad \Longleftrightarrow \quad 0 = \sum_{k \neq j} \gamma_k \frac{\xi_j - \xi_k}{|\xi_j - \xi_k|^2} - \omega \xi_j$$

PHYSICAL REVIEW E, VOLUME 64, 011603

Dynamic, self-assembled aggregates of magnetized, millimeter-sized objects rotating at the liquid-air interface: Macroscopic, two-dimensional classical artificial atoms and molecules

Bartosz A. Grzybowski,[1] Xingyu Jiang,[1] Howard A. Stone,[2] and George M. Whitesides[1,*]
[1]*Department of Chemistry and Chemical Biology, Harvard University, 12 Oxford Street, Cambridge, Massachusetts 02138*
[2]*Division of Engineering and Applied Sciences, Harvard University, Pierce Hall, Cambridge, Massachusetts 02138*
(Received 3 October 2000; published 21 June 2001)

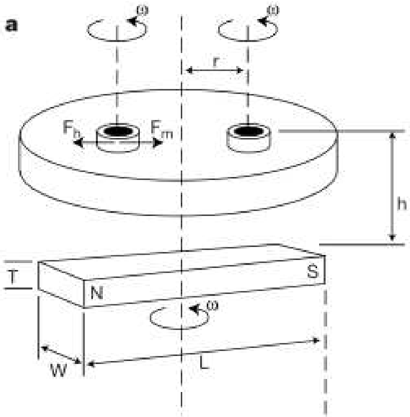

ure 1 Experimental set-up and magnetic force profiles. **a**, A scheme of the ›erimental set-up. A bar magnet rotates at angular velocity ω below a dish filled with ıid (typically ethylene glycol/water or glycerine/water solutions). Magnetically doped ‹s are placed on the liquid–air interface, and are fully immersed in the liquid except for ir top surface. The disks spin at angular velocity ω around their axes. A magnetic force attracts the disks towards the centre of the dish, and a hydrodynamic force F pushes

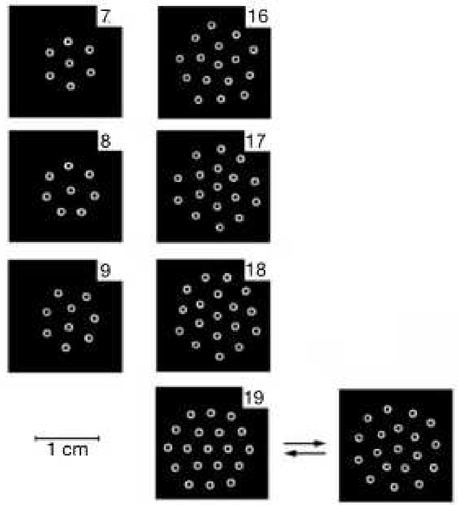

Figure 2 Dynamic patterns formed by various numbers (n) of disks rotating at the ethylene glycol/water–air interface. This interface is 27 mm above the plane of the external magnet. The disks are composed of a section of polyethylene tube (white) of outer diameter 1.27 mm, filled with poly(dimethylsiloxane), PDMS, doped with 25 wt% of magnetite (black centre). All disks spin around their centres at ω = 700 r.p.m., and the entire aggregate slowly ($\Omega < 2$ r.p.m.) precesses around its centre. For $n < 5$, the aggregates do not have a 'nucleus'—all disks are precessing on the rim of a circle. For $n > 5$, nucleated structures appear. For $n = 10$ and $n = 12$, the patterns are bistable in the sense that the two observed patterns interconvert irregularly with time. For $n = 19$, the hexagonal pattern (left) appears only above $\omega \approx$ 800 r.p.m., but can be 'annealed' down

Observation of Vortex Lattices in Bose-Einstein Condensates

20 APRIL 2001 VOL 292 SCIENCE

J. R. Abo-Shaeer, C. Raman, J. M. Vogels, W. Ketterle

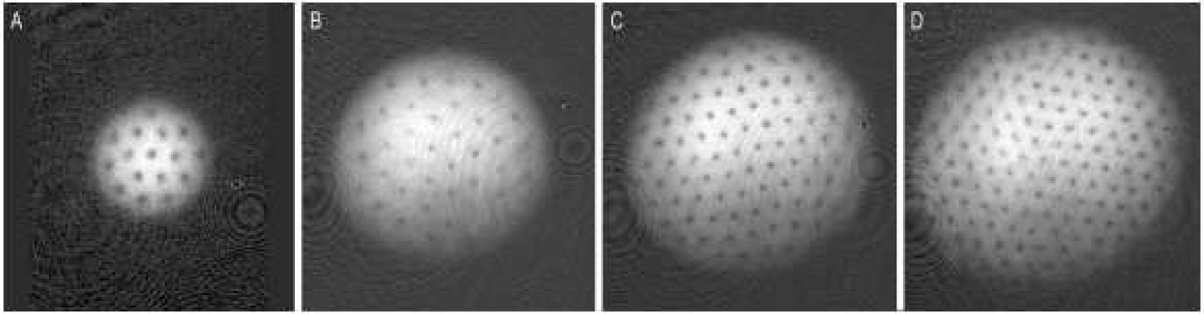

Fig. 1. Observation of vortex lattices. The examples shown contain approximately (**A**) 16, (**B**) 32, (**C**) 80, and (**D**) 130 vortices. The vortices have "crystallized" in a triangular pattern. The diameter of the cloud in (D) was 1 mm after ballistic expansion, which represents a magnification of 20. Slight asymmetries in the density distribution were due to absorption of the optical pumping light.

- Campbell and Ziff (1978) classified many stable configurations for ***small*** $(eg.\ N = 18)$ number of vortices of equal strength.

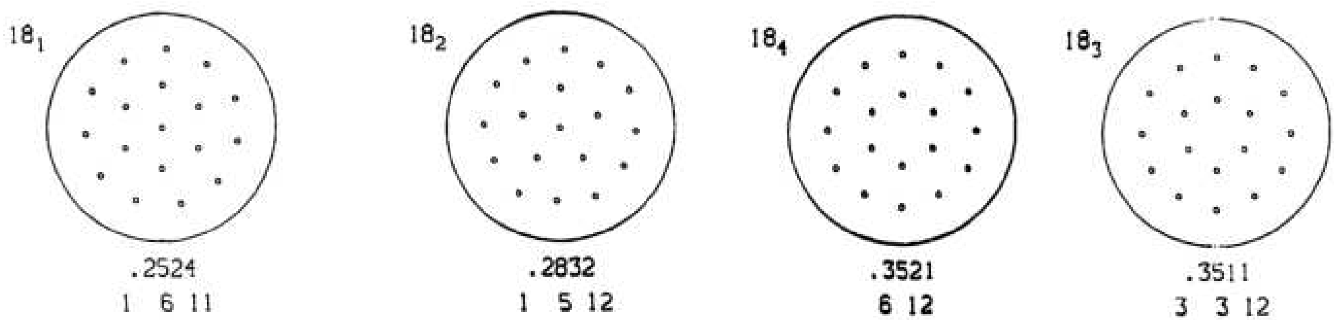

- Goal: describe the stable configuration in the continuum limit of a ***large*** number of vortices N (eg. $N = 100,\ 1000\ldots$). These have been observed in several recent expriments: Bose Einstein Condensates, magnetized disks

Key observation

$$\text{Vortex model: } \frac{dz_j}{dt} = i \sum_{k \neq j} \gamma_k \frac{z_j - z_k}{|z_j - z_k|^2}, \quad j = 1 \ldots N. \tag{V}$$

$$\text{Relative equilibrium: } z_j(t) = e^{\omega i t}\xi_j \quad \Longleftrightarrow \quad 0 = \sum_{k \neq j} \gamma_k \frac{\xi_j - \xi_k}{|\xi_j - \xi_k|^2} - \omega \xi_j$$

$$\text{Aggregation model: } \frac{dx_j}{dt} = \sum_{k \neq j} \gamma_k \frac{x_j - x_k}{|x_j - x_k|^2} - \omega x_j. \tag{A}$$

- One-to-one correspondence between the steady statates $x_j(t) = \xi_j$ of (A) and the relative equilibrium $z_j(t) = e^{\omega i t}\xi_j$ of (V).
- ***Spectral equivalence of (V) and (A):*** The equilibrium $x_j(t) = \xi_j$ is asymptotically stable for the aggregation model (A) if and only if the relative equilibrium $z_j(t) = e^{\omega i t}\xi_j$ is stable (neutrally, in the Hamiltonian sense) for the vortex model (V)!
- Aggregation model fully describes relative equilibria and their linear stability in the vortex model.
- Aggregation model is easier to study than the vortex model.

Vortices of equal strength $\gamma_k = \gamma$

Corresponding aggregation model:

$$\frac{dx_j}{dt} = \sum_{k \neq j} \gamma \frac{x_j - x_k}{|x_j - x_k|^2} - \omega x_j. \tag{23}$$

- Coarse-grain by defining the particle density to be

$$\rho(x) = \sum_{k=1 \dots N} \delta(x - x_k). \tag{24}$$

Then (23) is equivalent to $\dot{x}_j = v(x_j)$ where

$$v(x) \equiv -\omega x + \gamma \int_{\mathbb{R}^2} \frac{x-y}{|x-y|^2} \rho\,(y)\, dy, \tag{25}$$

and density is subject to conservation of mass

$$\rho_t + \nabla \cdot (\rho v) = 0. \tag{26}$$

- [Fetecau&Huang&Kolokolnikov2011]: In the limit $N \to \infty$, the steady state density of (A) is constant inside the ball of radius

$$R_0 = \sqrt{N\gamma/\omega}.$$

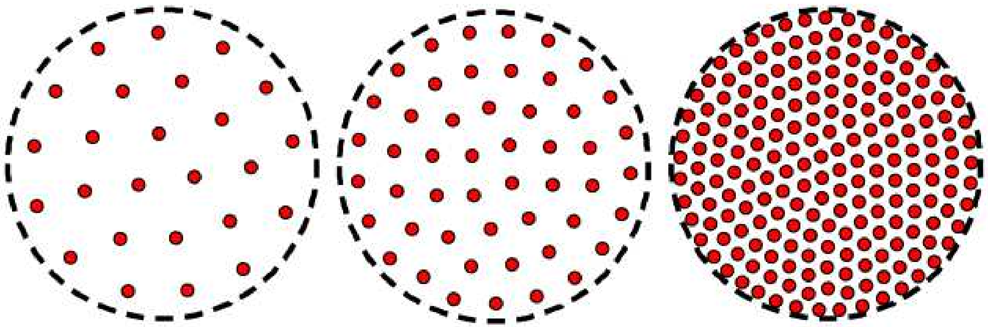

Fig. 1. Stable relative equilibria of $N = 25, 50$ and 200 vortices of equal strength. The dashed line shows the analytical prediction $R_0 = \sqrt{N\gamma/\omega}$ of the swarm radius in the $N \to \infty$ limit (see (6)).

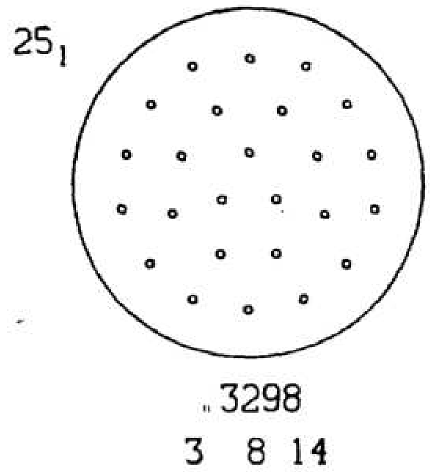

Crystallization

$$\text{Vortex model: } \frac{dz_j}{dt} = i \sum_{k \neq j} \gamma_k \frac{z_j - z_k}{|z_j - z_k|^2}, \quad j = 1 \ldots N. \tag{V}$$

$$\text{Reltive equiliria: } z_j(t) = e^{\omega i t} \xi_j \quad \Longleftrightarrow \quad 0 = \sum_{k \neq j} \gamma_k \frac{\xi_j - \xi_k}{|\xi_j - \xi_k|^2} - \omega \xi_j$$

$$\text{Vortex with dissipation: } \frac{dz_j}{dt} = i \sum_{k \neq j} \gamma_k \frac{z_j - z_k}{|z_j - z_k|^2} + \mu \left(\sum_{k \neq j} \gamma_k \frac{z_j - z_k}{|z_j - z_k|^2} - \omega z_j \right) \tag{D}$$

- In many physical experiments of BEC there is damping or dissipation involved.
- ***Spectral equivalence:*** Relative equilibria ***and their stability*** are the same for (V) and (D)
- Both the vortex model and the “aggregation model” model are limiting cases of (D).
- Taking $\mu > 0$ ***stabilizes vortex dynamics!*** $chaos\ damped\ stable$
- This allows us to find stable relative equilibria numerically.

Vortex dynamics in BEC with trap

- For BEC, dynamics have extra term corresponding to prcession around the trap:

$$\dot{z}_j = \underbrace{i\frac{a}{1-r^2}}_{\text{trap-interaction}} z_j + \underbrace{ic\sum_{k\neq j}\frac{z_j - z_k}{|z_j - z_k|^2}}_{\text{self-interaction}}, \quad j = 1 \ldots N. \tag{27}$$

- Large N limit:

$$v(x) \equiv (f(r) - \omega)\, x + c\int_{\mathbb{R}^2} \frac{x-y}{|x-y|^2}\rho(y)\, dy.$$

$$\int_{\mathbb{R}^2} \rho(x)dx = N,$$

- ***Non-uniform*** vortex lattice state:

$$\rho \sim \frac{1}{\pi c}\left(\omega - \frac{a}{(1-r^2)^2}\right) \text{ if } r < R, \quad \rho = 0 \text{ otherwise,}$$

with $\omega = \dfrac{a}{1-R^2} + \dfrac{cN}{R^2}$

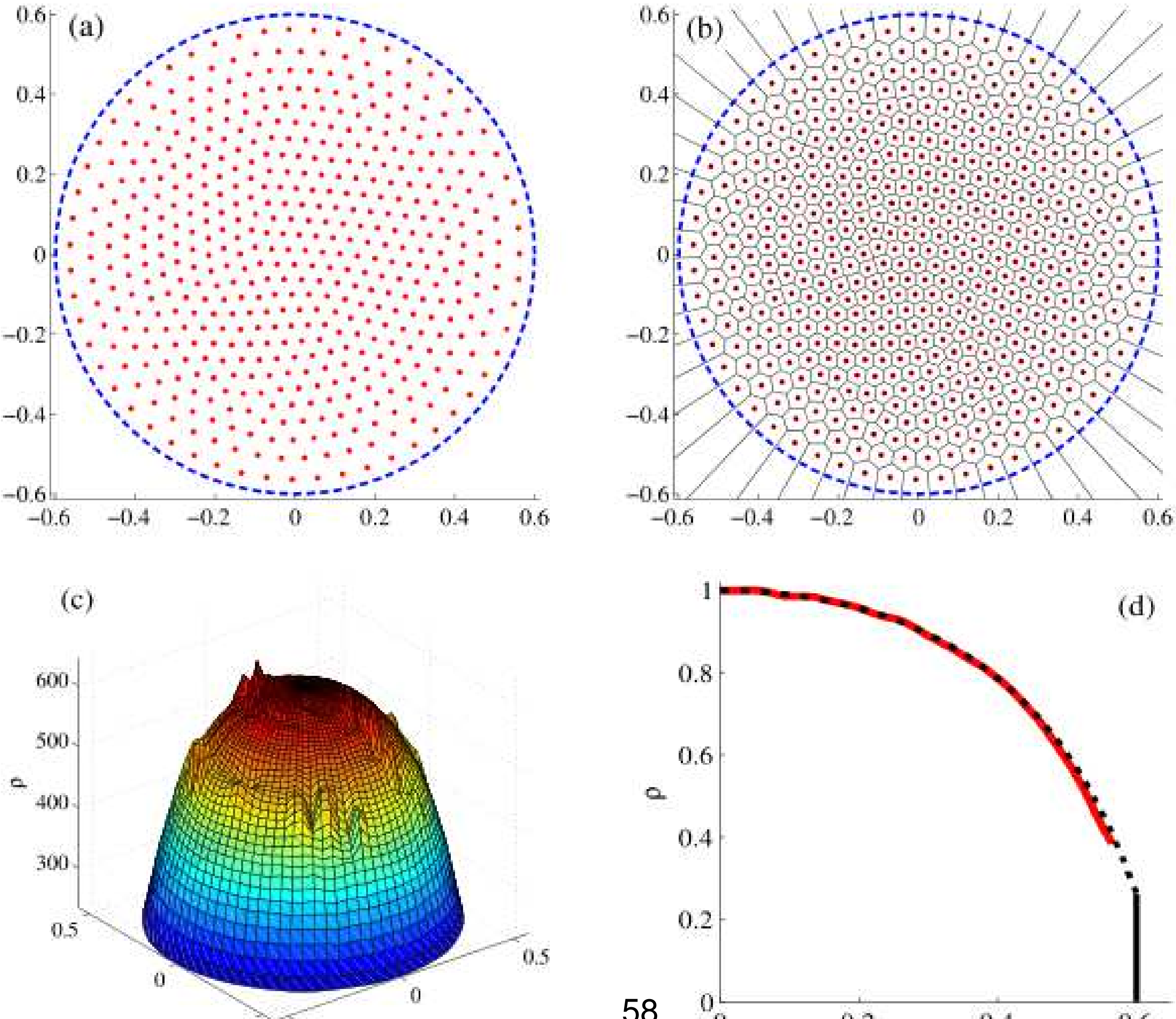

(a)
(b)
(c)
(d)
ρ

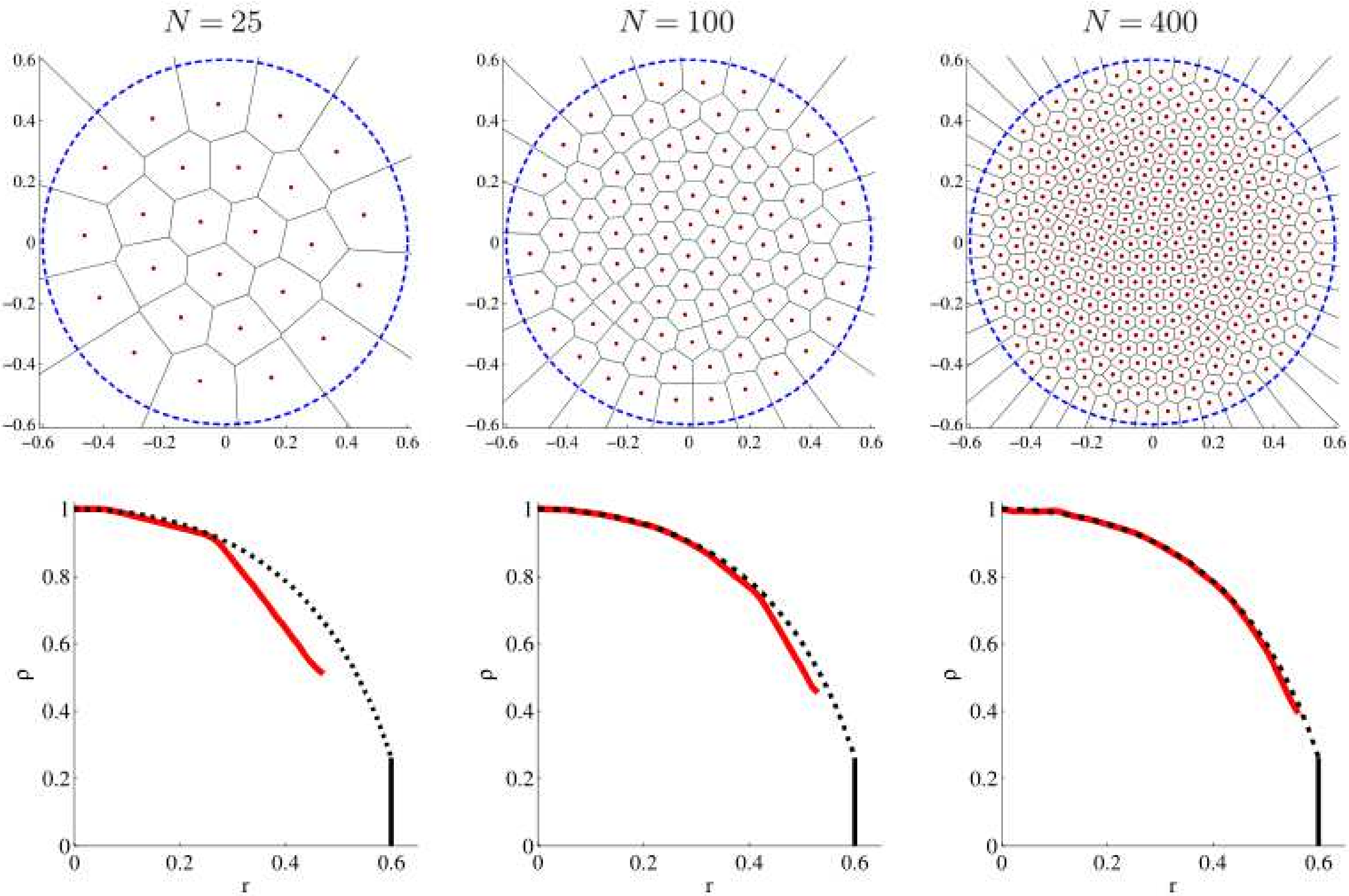

Figure 2. Top row: stable equilibrium of Eq. (2.4) with $f(r)$ as in Eq. (2.2), with N as shown in the title and with $c = 0.5/N$, $\omega = 2.95139$, $a = 1$. The dashed circle is the asymptotic boundary whose radius $R = 0.6$ is the smaller solution to Eq. (4.9). Bottom row: average of $\rho(|x|)/\rho(0)$ as a function of $r = |x|$. Solid curve corresponds to the numerical computation. Dashed curve is the formula (4.10). Vertical line is the boundary $r = R$.

Maximum N

$$\omega_c = \left(\sqrt{a} + \sqrt{cN}\right)^2; \quad R_c^2 = \frac{\sqrt{cN}}{\sqrt{a} + \sqrt{cN}}.$$

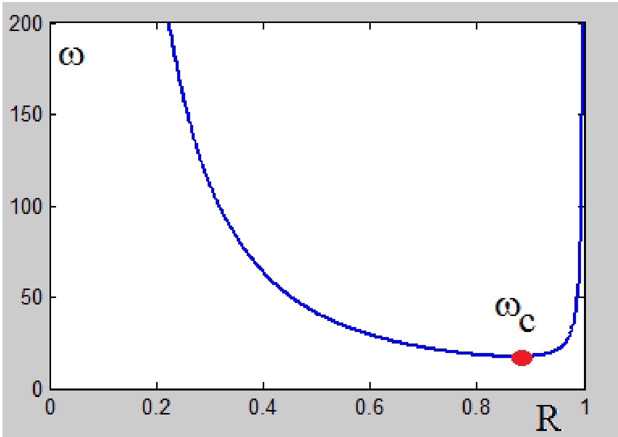

- No solutions if $\omega < \omega_c$
- Two solutions $R = R_\pm$ if $\omega > \omega_c$
  - smaller is stable, larger has negative density (unphysical).
- Corrollary: must have $N < N_{\max}$ where

$$N_{\max} = \frac{\left(\sqrt{\omega} - \sqrt{a}\right)^2}{c}. \tag{28}$$

$N + 1$ problem

- N vortices of equal strength and a single vortex of a much higher strength:

$$\frac{dx_j}{dt} = \frac{a}{N} \sum_{\substack{k=1\dots N \\ k\neq j}} \frac{x_j - x_k}{|x_j - x_k|^2} + b\frac{x_j - \eta}{|x_j - \eta|^2} - x_j, \quad j = 1\dots N, \tag{29}$$

$$\frac{d\eta}{dt} = \frac{a}{N} \sum_{k=1\dots N} \frac{\eta - x_k}{|\eta - x_k|^2} - \eta \tag{30}$$

- Mean-field limit $N \to \infty$:

$$\begin{cases} \rho_t + \nabla \cdot (\rho \nabla v) = 0; \\ v(x) = a \int_{\mathbb{R}^2} \rho(y) \frac{x-y}{|x-y|^2} dy + b\frac{x-\eta}{|x-\eta|^2} - x \\ \frac{d\eta}{dt} = a \int_{\mathbb{R}^2} \rho(y) \frac{\eta - y}{|\eta - y|^2} dy - \eta \end{cases}. \tag{31}$$

- **Main result:**. Define $R_1 = \sqrt{b}$, $R_0 = \sqrt{a+b}$ and suppose that η is any point such that $B_{R_1}(\eta) \subset B_{R_0}(0)$. Then the equilibrium solution for (31) is constant inside $B_{R_0}(0) \backslash B_{R_1}(\eta)$ and is zero outside.

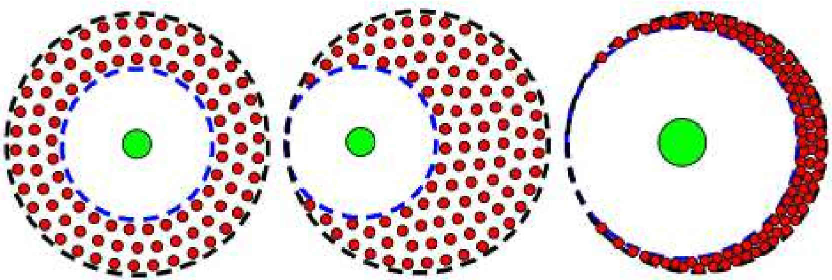

- Unlike the $N+0$ problem, the relative equilibrium for the $N+1$ problem is non-unique: any choice of η yields a steady state as long as $|\eta| < R_0 - R_1$.

Degenerate case: big central vortex

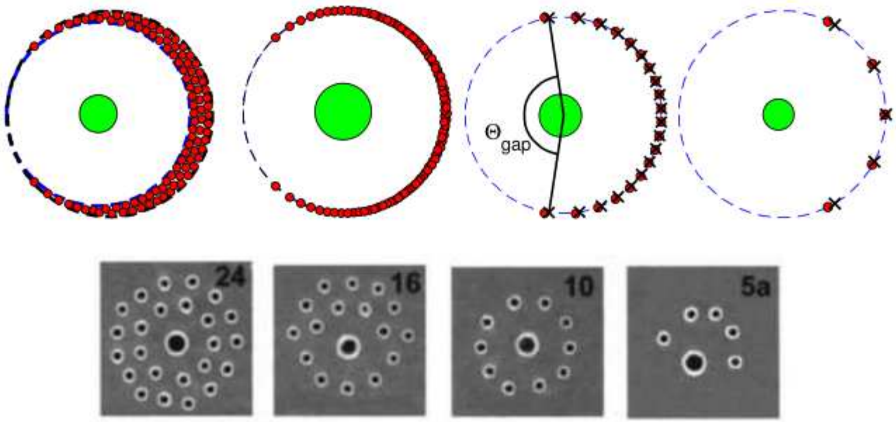

- Small vortices are constrained to a ring of radius R_0. with big vortex at the center.
- ***Non-uniform*** distribution of small particles!
- Question: Determine the size of the gap Θ_{gap}.

- **Main Result:**

$$\Theta_{gap} \sim CN^{-1/3}.$$

where the constant $C = 8.244$ satisfies

$$\left(8 - 6u + 2u^3\right) \ln\left(u - 1\right) = 3u\left(u^2 - 4\right); \quad C = 2\left(\frac{6\pi(2-u)}{u\left(u^2-1\right)}\right)^{1/3}$$

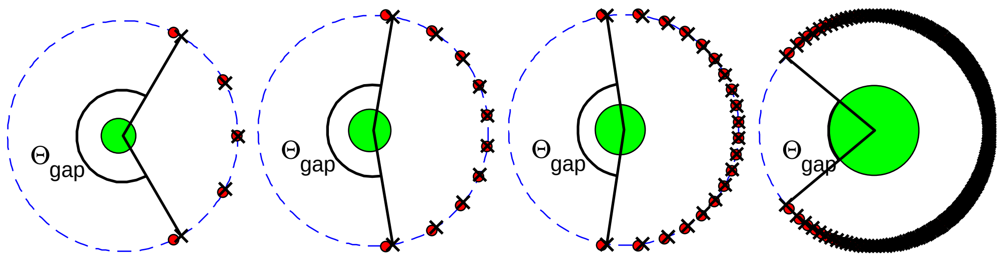

Sketch of proof

- [Barry+Wayne, 2012]: Set $x_j(t) \sim R_0 e^{i\theta_j(t)}$ then at leading order we get

$$\frac{d\theta_j}{dt} = \frac{1}{N}\sum_{k\neq j}\left(\frac{\sin\left(\theta_j - \theta_k\right)}{2 - 2\cos\left(\theta_j - \theta_k\right)} - \sin\left(\theta_j - \theta_k\right)\right). \tag{32}$$

- In the mean-field limit $N \to \infty$, the density distribution $\rho(\theta)$ for the angles θ_j satisfies

$$\begin{cases} \rho_t + \left(\rho v_\theta\right)_\theta = 0, \\ v(\theta) = PV \displaystyle\int_{-\pi}^{\pi} \rho\left(\phi\right)\left(\frac{\sin\left(\theta - \phi\right)}{2 - 2\cos\left(\theta - \phi\right)} - \sin\left(\theta - \phi\right)\right) d\phi, \end{cases} \tag{33}$$

  where PV denotes the principal value integral, and $\int_{-\pi}^{\pi} \rho = 1$.

- [Barry, PhD Thesis]: Up to rotations, the steady state density $\rho(\theta)$ for which $v = 0$ must be of the form

$$\rho(\theta) = \frac{1}{2\pi}\left(1 + \alpha\cos\theta\right). \tag{34}$$

  This follows from (33) and (formal) expansion

$$\frac{\sin t}{2 - 2\cos t} - \sin t = \sin(2t) + \sin(3t) + \sin(4t) + \dots$$

- α is free parameter in the continuum limit.

- For discrete N, particle positions satisfy

$$\int_{\theta_{j-1}}^{\theta_j} \frac{1}{2\pi} (1 + \alpha \cos\theta)\, d\theta = \frac{1}{N}$$

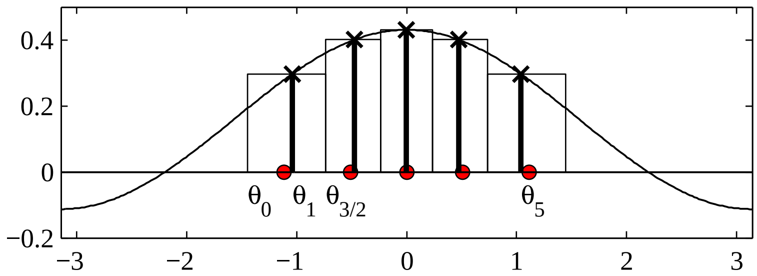

To estimate Φ_{gap}, choose θ_1 so that $v(\theta_1) \sim 0$. See our paper for hairy details.

$N + K$ problem

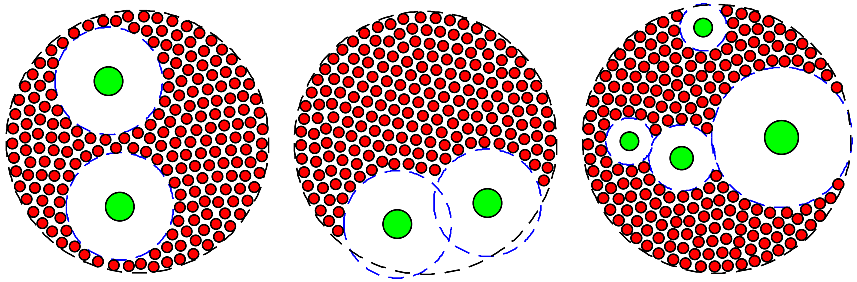

$$v(x) = a\int_{\mathbb{R}^2} \rho(y)\frac{x-y}{|x-y|^2}dy + \sum_{k=1\ldots K} b_k \frac{x-\eta_k}{|x-\eta_k|^2} - x,$$

$$\frac{d\eta_j}{dt} = a\int_{\mathbb{R}^2} \rho(y)\frac{\eta_k-y}{|\eta_k-y|^2}dy + \sum_{\substack{k=1\ldots K\\ k\neq j}} b_k \frac{\eta_j-\eta_k}{|\eta_j-\eta_k|^2} - \eta_j,$$

$$j = 1\ldots K.$$

Main result: Let $R_k = \sqrt{b_k},\quad k = 1\ldots K$ and $R_0 = \sqrt{a+b_1+\ldots+b_K}$. Suppose $\eta_1\ldots\eta_K$ are such $B_{R_1}(\eta_1)\ldots B_{R_K}(\eta_K)$ are all disjoint and are contained inside $B_{R_0}(0)$. The equilibrium density is constant inside $B_{R_0}(0)\backslash\bigcup_{k=1}^K B_{R_k}(\eta_k)$ and is zero outside.

$N + K$ problem, with very large K vortices

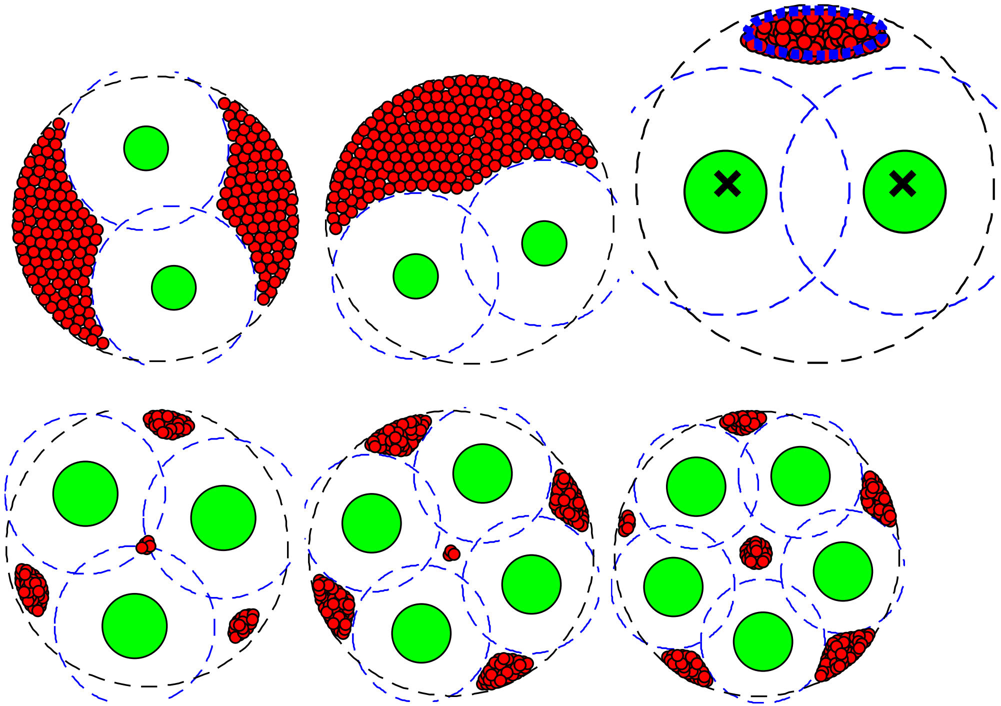

- The ***blue ellipse*** is described by the reduced system

$$\frac{d\xi_j}{dt} = \frac{1}{N} \sum_{\substack{k=1...N \\ k\neq j}} \frac{1}{\overline{\xi_j - \xi_k}} + \frac{1}{2}\bar{\xi}_k - \xi_k \tag{35}$$

- From [K, Huang, Fetecau, 20011], its axis ratio is 3.